

Specialization of softmax attention heads: insights from the high-dimensional single-location model.

Margarita Sagitova, Odilon Duranthon, and Lenka Zdeborová*
*Statistical physics of computation laboratory,
École Polytechnique Fédérale de Lausanne, Switzerland*

Multi-head attention enables transformer models to represent multiple attention patterns simultaneously. Empirically, head specialization emerges in distinct stages during training, while many heads remain redundant and learn similar representations. We propose a theoretical model capturing this phenomenon, based on the multi-index and single-location regression frameworks. In the first part, we analyze the training dynamics of multi-head softmax attention under SGD, revealing an initial unspecialized phase followed by a multi-stage specialization phase in which different heads sequentially align with latent signal directions. In the second part, we study the impact of attention activation functions on performance. We show that softmax-1 significantly reduces noise from irrelevant heads. Finally, we introduce the Bayes-softmax attention, which achieves optimal prediction performance in this setting.

I. INTRODUCTION

Multi-head attention is a central architectural ingredient of modern transformer models, enabling multiple attention patterns to coexist within a single layer. Empirical analyses show that attention heads do not all develop simultaneously during training: instead, new specialized heads emerge in distinct stages, with qualitatively new attention behaviors appearing as training progresses [1–5]. At the same time, a substantial fraction of heads in trained models remain redundant and can be removed with little impact on performance [6, 7]. These observations raise a natural theoretical question: what drives staged head emergence and persistent redundancy in multi-head attention?

Recent theoretical work has begun to elucidate training dynamics and head specialization in simplified attention models. In in-context learning of linear regression, linear attention exhibits saddle-to-saddle dynamics in which heads sequentially align with covariance eigenmodes of the data distribution [8], while multi-head softmax attention in multi-task linear regression displays short emergence phases during which different heads align with distinct tasks and converge to optimal predictors [9]. These analyses establish in-context linear regression as a first solvable setting in which head specialization can be studied from first principles. At the same time, attention mechanisms are deployed in a broad range of architectures and data regimes where the structure of the learning problem and the role of redundant heads may differ. Developing a variety of solvable models is therefore essential to identify which aspects of head specialization and redundancy are universal and which depend on architectural and statistical details. In particular, regimes where multi-head attention itself constitutes the sole predictive mechanism and head outputs are uniformly aggregated raise new questions about how attention normalization interacts with specialization and redundancy.

In this work, we study head specialization in a controlled high-dimensional setting by specifying both a probabilistic data model and a minimal attention architecture trained on it. We consider a synthetic sequence-to-token regression task in which one token carries structured signal generated from a multi-index latent model, while all other tokens contain pure noise. The task is to recover the relevant token from the sequence, making attention a natural mechanism for the problem. We learn this task with a multi-head softmax attention layer trained by stochastic gradient descent, whose head outputs are uniformly aggregated so that attention itself constitutes the sole predictive mechanism.

This yields a minimal setting in which redundant heads can inject persistent variance if they fail to specialize, making attention normalization a central modeling ingredient. Our setting also connects to classical committee-machine and multi-index models: the multi-head architecture plays the role of a committee in which each head acts as a unit with its own parameters, and specialization corresponds to symmetry breaking among these units under SGD [10–13]. It is likewise related to recent high-dimensional analyses of SGD in multi-index and sequence single-index models [14–18]. Our model is also closely related to recent solvable attention and sequence regression frameworks [19–23], which analyze high-dimensional training dynamics of simplified attention architectures from first principles.

Within the considered setting, in the high-dimensional limit, the evolution of the attention parameters reduces to a low-dimensional system of order parameters tracking head alignments and overlaps with the latent signal structure. This analysis reveals a two-stage learning dynamics: an initial fast phase where heads develop a common component

* firstname.secondname@epfl.ch

aligned with the easiest (mean) signal direction, followed by a slower specialization phase in which different heads diverge and align with additional latent directions of the signal. The hierarchy of these specialization events is governed by the latent signal structure, leading to sequential acquisition of increasingly subtle components (see also [24] for stagewise learning in deep linear networks).

We further study how attention activation functions allowing some heads to be effectively deactivated influence the model performance. In our minimal architecture, redundant or poorly specialized heads can inject persistent variance, making attention normalization a central modeling ingredient. Alternative attention activations or extra sink tokens have previously been investigated mainly to prevent over-focusing on irrelevant tokens [25–27]. Here, we analyze such activations as tools for controlling head redundancy and specialization. Finally, [28] showed that head-specific gating of attention outputs enhances performance, motivating the study of deactivation mechanisms without additional parameters.

Our main contributions are as follows.

- (i) We introduce a high-dimensional probabilistic framework for training multi-head softmax attention in a sequence-to-token regression task, enabling an exact characterization of learning dynamics under stochastic gradient descent.
- (ii) We derive a closed system of equations describing the evolution of head alignments and overlaps, and show that training exhibits a fast unspecialized phase followed by a slower hierarchy of specialization events governed by the latent signal structure.
- (iii) We analyze the effect of attention normalization on head redundancy, proving that standard softmax is generically suboptimal in this setting, while alternative activations such as softmax-1 mitigate variance induced by redundant heads. We introduce the Bayes-softmax attention, which, in our setting, reaches the Bayes-risk and prescribes the optimal number of heads and the way to normalize them.

Notations

For a positive integer n we write $[n] = \{1, \dots, n\}$. We use $\delta_{i,j}$ to denote a Kronecker delta that evaluates to 1 if $i = j$ and 0 otherwise. For a vector v , $v^{\odot 2}$ is the element-wise square, $\text{Diag}(v)$ the diagonal matrix which diagonal is v . For a positive integer n , $\mathbf{1}_n \in \mathbb{R}^n$ is the vector filled with ones, I_n the $n \times n$ identity matrix, \mathcal{S}_+^n is the set of positive symmetric $n \times n$ matrices. For a matrix A , A_i is the vector made by its i -th row and $A_{\cdot i}$ by its i -th column. $\|\cdot\|_2$ is the L_2 norm of a vector, $\|\cdot\|_F$ is the Frobenius norm of a matrix. We denote a Gaussian law centered at ω with covariance V as $\mathcal{N}(\omega, V)$.

II. TASK AND DATA MODEL

We denote a sequence $X \in \mathbb{R}^{L \times D}$ made of L tokens of dimension D . We choose a relevant token X_ϵ by setting a hidden index $\epsilon \in [L]$. This models the fact that, in transformers, the attention is often used to focus and extract one particular token that is needed by the subsequent layers. The relevant token is distinguished from the other tokens by a planted hidden spike $\hat{k} \in \mathbb{R}^D$. We emphasize that the latent ϵ and \hat{k} are different in every sequence/context. Hence their recovery is akin to a toy in-context learning (ICL) task.

A. Probabilistic model of data

Inspired by [19, 20], we introduce a probabilistic data model for this task, that is amenable to analysis in the high-dimensional limit. To define it we begin by drawing F hidden spikes

$$k_f^* \sim \mathcal{N}(0, D^{-1}I_D) \quad \text{for } f \in [F]. \quad (1)$$

The hidden spikes are common to all the sequences. In the following, we may call them directions or features in an interchangeable manner. Each sequence $X \in \mathbb{R}^{L \times D}$ is then sampled as follows. The index ϵ of the relevant token is first taken uniformly at random over $\{1, \dots, L\}$. We take weights $\theta \in \mathbb{R}^F$ for the hidden directions/spikes/features according to a distribution P_θ . Then an effective sequence-dependent direction $\hat{k} \in \mathbb{R}^D$ is constructed as $\hat{k} = \sum_f^F \theta_f k_f^*$. The tokens and the label y are drawn according to

$$X_\ell \sim \mathcal{N}\left(\delta_{\ell, \epsilon} \hat{k}, I_D\right) \quad \text{for } \ell \in [L], \quad y = X_\epsilon. \quad (2)$$

The goal is, given X , to extract the relevant token y .

In the following we will consider different possible choices for P_θ , mainly focusing on:

Flipping spike. For $F = 2$ and signal strengths $\nu_1 > 0, \nu_2 > 0$, $\theta_1 = \sqrt{\nu_1}$ is a constant direction while $\theta_2 \sim \text{Unif}(\{-\sqrt{\nu_2}, +\sqrt{\nu_2}\})$ alternates. For $F > 2$ and signal $\nu > 0$, we take $\theta \sim \text{Unif}(\{\sqrt{\nu}e_f\}_{f \in [F]})$ with $\{e_f\}_{f \in [F]}$ the canonical basis of \mathbb{R}^F .

Non-isotropic Gaussian. For any F and two signal strengths $\nu_1 \geq \nu_2 > 0$, we take $\theta_f \sim \mathcal{N}(0, \tilde{\nu}_f)$ for all f , with $\tilde{\nu}_1 \geq \tilde{\nu}_2 \geq \dots \geq \tilde{\nu}_F$ linearly scaled between ν_1 and ν_2 . This allows for different signal strengths for the different features. The particular case $\nu_1 = \nu_2 := \nu$ corresponds to the **isotropic Gaussian**.

B. Learning with attention

We consider the class of estimators $\mathcal{F}_\sigma = \{\hat{y}_{\sigma,k,b,v} : \mathbb{R}^{L \times D} \rightarrow \mathbb{R}^D\}_{k \in \mathbb{R}^{H \times D}, b \in \mathbb{R}^H, v \in \mathbb{R}}$ where for H vectors $k_1, \dots, k_H \in \mathbb{R}^D$, H scalar biases b_1, \dots, b_H , a scalar v and an activation function $\sigma : (\mathbb{R}^{H \times L}, \mathbb{R}^H, \mathbb{R}, [H]) \rightarrow \mathbb{R}^L$, the function $\hat{y}_{\sigma,k,b,v}$ is defined by

$$\hat{y}_{\sigma,k,b,v}(X) = \frac{1}{H} \sum_h^H \sigma(\chi, b, v; h)^T X, \quad (3)$$

$$\chi_h = X k_h \in \mathbb{R}^L \quad \text{for } h \in [H].$$

This model can be viewed as a simplification of a cross-attention module where a query embedding is independent of the input sequence. Consider a single head attention layer with activation σ , scaling λ (which in practice is usually set to $1/\sqrt{D}$), key and query matrices $K, Q \in \mathbb{R}^{D \times p}$, value matrix is identity $V = I_D$, and let X_{query} be a query embedding independent of the input sequence $\text{Attn}_{\sigma,K,Q,V}(X) = \sigma(\lambda(XK)(Q^T X_{\text{query}}))^T X V = \sigma(\lambda \sum_{i=1}^p a_i (XK_{:i}))^T X$, where we denoted $Q^T X_{\text{query}} = a \in \mathbb{R}^p$ and $K_{:i} \in \mathbb{R}^D$ for $i = 1, \dots, p$ are the columns of the key matrix K . We effectively get attention scores that linearly depend on the input sequence, with the key-vector $k = \lambda \sum_{i=1}^p a_i K_{:i}$. Such attention is used, for example, in the decoder of DETECTION TRansformer [29], where input sequence represents encoded image patches and the query represents an object to detect. By analogy, our model is trained to find a patch in the ‘‘image’’ containing a specific ‘‘object’’ encoded by the spike, while all other patches in the sequence represent the ‘‘background’’ of the image.

As to the choice of the activation function we focus on the three following cases:

Softmax, which corresponds to the standard choice in current large language models. For a head h it is defined by $\sigma(\chi, b, v; h)_\ell = e^{\chi_{h\ell}} / \sum_{\ell'=1}^L e^{\chi_{h\ell'}}$. It does not depend on b or v and the heads only interact by summing their outputs.

Softmax-1, introduced in [25], defined by $\sigma(\chi, b, v; h)_\ell = v e^{\chi_{h\ell}} / (e^{b_h} + \sum_{\ell'=1}^L e^{\chi_{h\ell'}})$. Notice that the original article takes $e^{b_h} = 1$, which is equivalent to our formulation up to additional head-dependent biases in the attention scores. $\sum_\ell \sigma(\chi, b, v; h)_\ell$ can become smaller than 1, thus ‘‘deactivating’’ some heads. We allow a global rescaling by a factor v to compensate inactive heads.

Bayes-softmax (or B-softmax), motivated later, defined by

$$\sigma(\chi, b, v; h)_\ell = \frac{e^{\chi_{h\ell} + b_h}}{\frac{1}{H} \sum_{h'}^H \sum_{\ell'=1}^L e^{\chi_{h'\ell'} + b_{h'}}} \quad (4)$$

The B-softmax normalizes each head by the output of the H heads. It does not depend on v , but we allow for head-dependent biases.

The estimator \hat{y} is trained by SGD. The weights k_h are initialized at random $k_h \sim \mathcal{N}(0, \eta^2 D^{-1} I_D)$ with $\eta \in \mathbb{R}^+$ independent of D controlling the initial norm. The biases are initialized to 0 and v to 1. At time t the weight update is

$$\begin{aligned} k_h^{(t+1)} &= k_h^{(t)} - \gamma \nabla_{k_h^{(t)}} \mathcal{L}^{(t)} \quad \text{for } h \in [H] \\ b_h^{(t+1)} &= b_h^{(t)} - \gamma \nabla_{b_h^{(t)}} \mathcal{L}^{(t)} \quad \text{for } h \in [H] \\ v^{(t+1)} &= v^{(t)} - \gamma \nabla_{v^{(t)}} \mathcal{L}^{(t)} \end{aligned} \quad (5)$$

where $\gamma > 0$ is the learning rate and

$$\mathcal{L}^{(t)} = \frac{1}{N_b} \sum_{\mu=1}^{N_b} \frac{1}{D} \|y^{\mu,(t)} - \hat{y}_{\sigma,k^{(t)},b^{(t)},v^{(t)}}(X^{\mu,(t)})\|_2^2 \quad (6)$$

is the empirical loss over a batch of N_b sequences $\{(X^{\mu,(t)}, y^{\mu,(t)})\}_{\mu \in [N_b]}$ drawn iid according to the model eq. (2). We set $N = tN_b$ the total number of samples. Notice that, because of the independence of the batches, on average the estimator minimizes the population loss

$$\mathcal{E}_\sigma(k, b, v) = \frac{1}{D} \mathbb{E}_{X,y} [\|y - \hat{y}_{\sigma,k,b,v}(X)\|_2^2] . \quad (7)$$

III. DYNAMICS OF THE HEADS

We consider the limit of large embedding dimension $D \rightarrow \infty$ and constant sequence length, number of spikes, number of heads, signal strength and initialization, i.e., $L, F, H, \|\theta\|_2, \eta = \Theta(1)$. A first consequence of this limit is that the population loss \mathcal{E}_σ eq. (7) can be expressed in terms of a few *order parameters* (or *sufficient statistics*).

Proposition III.1 (Reparameterized loss). *The loss of the attention $(k, b, v) \mapsto \mathcal{E}_\sigma(k, b, v)$ can be reparameterized as a function $(m, r, b, v) \in (\mathbb{R}^{H \times F}, \mathcal{S}_+^H, \mathbb{R}^H, \mathbb{R}) \mapsto \tilde{\mathcal{E}}_\sigma(m, r, b, v)$ of the following order parameters, for $h, h' \in [H]$, $f, f' \in [F]$:*

$$m_{hf} = (k_h)^\top k_f^* \qquad q_{hh'} = (k_h)^\top k_{h'} \quad (8)$$

$$p_{ff'} = (k_f^*)^\top k_{f'}^* \qquad r = (q - mp^{-1}m^\top)^{1/2} \quad (9)$$

Let $\epsilon \sim \text{Unif}(\{1, \dots, L\})$, $\theta \sim P_\theta$ and conditionally on ϵ and θ , $\chi_\ell^* \sim \mathcal{N}(\delta_{\ell,\epsilon}\theta, I_F)$ and $\xi_\ell \sim \mathcal{N}(0, I_H)$ for $\ell \in [L]$. The reparameterized loss is

$$\tilde{\mathcal{E}}_\sigma(m, r, b, v) = \mathbb{E}_{\epsilon, \theta, \chi, \xi} \left[\sum_{\ell}^L \left(\delta_{\ell,\epsilon} - \frac{1}{H} \sum_h^H \sigma(\chi, b, v; h)_\ell \right)^2 \right] \quad (10)$$

$$\chi_{h\ell} = \sum_f^F m_{hf} \chi_{f\ell}^* + \sum_{h'}^H r_{hh'} \xi_{h'} \quad , \quad h \in [H], \ell \in [L] . \quad (11)$$

A derivation is given in Appendix A1. Here m_{hf} quantifies the alignment between the head h and the hidden direction f , while q is the overlap between the heads. r is the amplitude of the components that are orthogonal to the spikes; $r = 0$ whenever k is in the span of k^* . In our model, $p \approx I_F$ because the hidden directions are independently sampled from a high-dimensional normal distribution.

The motivation to introduce these order parameters is that the learning dynamics of the attention can be expressed in a closed-form over m and r . We consider the limit of gradient flow on the population loss, obtained by taking $\gamma N_b^{-1} = o(D^{-1})$ together with $N_b \geq 1$ and $\gamma = \mathcal{O}(1)$, as detailed e.g. in [30]. In particular, this encompasses the two following cases: i) large batches $N_b = \Theta(D)$ and vanishing learning rates $\gamma = o(1)$; and ii) constant-size batches $N_b = \Theta(1)$ and small learning rates $\gamma = o(D^{-1})$.

Proposition III.2 (Effective dynamics). *Consider the dynamics of SGD defined by eq. (5). Let $\tau = \gamma t$ be the effective time. Then, in the space of the order parameters the dynamics is given by*

$$\begin{aligned} \frac{\partial}{\partial \tau} m(\tau) &= -\nabla_m \tilde{\mathcal{E}}_\sigma(m(\tau), r(\tau), b(\tau), v(\tau)) \\ \frac{\partial}{\partial \tau} r(\tau) &= -\nabla_r \tilde{\mathcal{E}}_\sigma(m(\tau), r(\tau), b(\tau), v(\tau)) \end{aligned} \quad (12)$$

and $\partial_\tau b = -\nabla_b \tilde{\mathcal{E}}_\sigma$ and $\partial_\tau v = -\nabla_v \tilde{\mathcal{E}}_\sigma$.

Similar results, on the equivalence between the dynamics of SGD in the high-dimensional space and the space of order parameters, have been derived for fully-connected two-layer neural networks in e.g. [12, 16, 17, 30] and in [18] for sequence single-index models; a proof of this result for our model would follow the same steps. As a numerical check, we provide simulations in Fig. 1 and in Figs. 9 and 10 in Appendix. The agreement between the theory and the simulations is very good.

A consequence of Prop. III.2 is the characterization of two distinct phases in the learning. At random initialization m concentrates around 0. In the first phase, the heads do not specialize and move collectively towards the mean of the signal in a few time steps. The dynamics is controlled by the gradient of the loss in the direction of the mean signal.

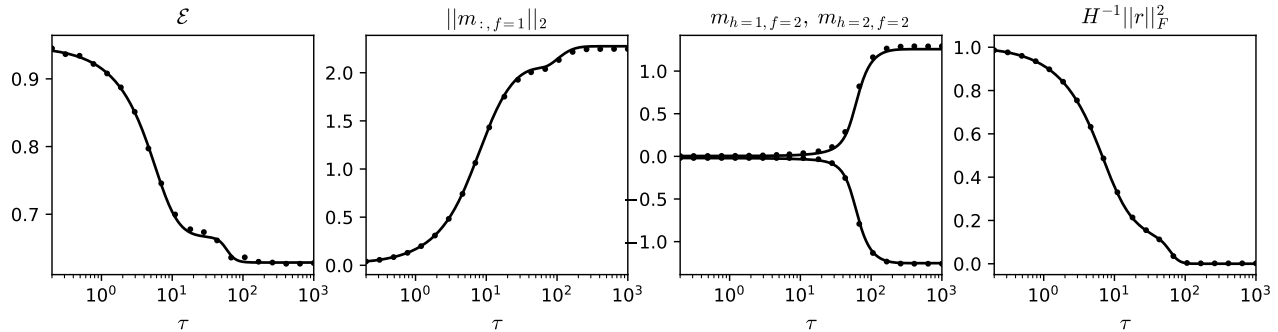


FIG. 1. Asymptotic description of the attention trained by SGD. We compare numerical simulations at finite $D = 10^4$ (dots) and the theoretical description stated in proposition III.2 (continuous lines). We consider sequence length $L = 10$, $H = 2$ heads with σ softmax attention, $F = 2$ features, θ drawn from the flipping spike distribution, with signal strengths $\nu_1 = \nu_2 = 2$. $f = 1$ is the “constant” direction while $f = 2$ is the “flipping sign” direction. Initialization $\eta = 1$.

Proposition III.3 (Unspecialized phase). *Let $\mathbb{E}\theta = (\mathbb{E}_{P_\theta} \theta_f)_{f \in [F]} \in \mathbb{R}^F$ be the mean of the feature weights and assume it does not vanish $\mathbb{E}\theta \neq 0$. There is a finite time $\tau^u = \Theta(1)$ for which there is a $x \in \mathbb{R}^+$, $x = \Theta(1)$ such that, for all $h \in [H]$, $m_h(\tau^u) = x\mathbb{E}\theta + \mathcal{O}(D^{-1/2})$.*

This result comes from the facts that the space of unspecialized m , r and b is invariant by the gradient flow, as stated in Lemma A.1, and that at $m = 0$ the gradient does not vanish and points towards $\mathbb{E}\theta$, as stated in Lemma A.2 in Appendix A 2 b. Learning the mean direction $\mathbb{E}\theta$ is fast and in total it requires N larger than $\Theta(D)$ samples to recover this direction. This is depicted in Fig. 1, where we consider the flipping sign distribution, where $\mathbb{E}\theta_1 > 0$ and $\mathbb{E}\theta_2 = 0$. In the 2nd panel, a time $\tau^u \approx 1$ is enough to start learning the direction $f = 1$. In the case when $\mathbb{E}\theta = 0$, m does not move until the next phase. The biases b stay unspecialized: around τ^u there is $\tilde{b} \in \mathbb{R}$ such that $b_h = \tilde{b}$ for all h , with for the B-softmax $\tilde{b} = 0$ and for the softmax-1 \tilde{b} such that on average the output of the attention scales to 1.

The specialization of the heads can occur only in the second phase after the unspecialized phase. It requires the presence of a descent direction orthogonal to $\mathbb{E}\theta$. As shown by Lemma III.1 and as justified in Appendix A 2 a, this condition is fulfilled in particular for $\|\mathbb{E}\theta\|_2$ small enough and small enough initialization η , the limit being taken after $D \rightarrow \infty$. We numerically checked that it holds more generally for all the choices of parameters we consider in this article.

Proposition III.4 (Specialization phase). *Let $P_{\perp \mathbb{E}\theta}$ be the projection onto the space orthogonal to $\mathbb{E}\theta$. Assume that $P_{\perp \mathbb{E}\theta} \text{Cov}(\theta) P_{\perp \mathbb{E}\theta}^\top$ is not fully degenerated. Assume that $\|\mathbb{E}\theta\|_2$ and η are small enough, independently of D . There is a time $\tau^s = \Theta(\log D)$ at which, for all $h \in [H]$, $\|P_{\perp \mathbb{E}\theta} m_h(\tau^s)\|_2 = \Theta(1)$. Moreover, the heads start specializing: $\|m_h - m_{h'}\|_2 = \Theta(1)$ for some $h \neq h'$.*

A justification of this result is given in App. A 2 a. Learning the directions orthogonal to $\mathbb{E}\theta$ and specializing the heads is slower and in total it requires N larger than $\Theta(D \log D)$ samples to start specializing. As depicted in Fig. 1, 3rd panel, time $\tau^s \approx 10$ is needed at $D = 10^4$, during which the alignment with the orthogonal direction and the difference between the heads plateau at 0. τ^s is the time needed to escape the saddle at $P_{\perp \mathbb{E}\theta} m = 0$; its precise value depends on the details of the initialization $P_{\perp \mathbb{E}\theta} m(\tau = 0)$ and varies between runs. In particular, to obtain a match between the theory and the simulation one has to initialize m and r to their empirical values at $\tau = 0$. Notice that even though Prop. III.4 is derived for small $\|\mathbb{E}\theta\|_2$ and small η , it holds for larger values, as shown numerically by Figs. 1 to 4 and in Appendix C 1.

These two stages are further illustrated in Fig. 2 for the flipping sign distribution, for different H , where we see that in the first phase of training, all the heads align with the constant direction, and only after some time do they begin to diverge along the “flipping sign” direction. When increasing the number of heads, some heads specialize and diverge more from the average direction. The specialization of the heads versus the two signal strengths and versus H is further numerically analyzed in Appendices C 2 and C 3 a respectively.

A. Sequential specialization

We give insights on how the specialization of the heads occurs during this second phase. The dynamics depends on the initial condition $k^{(0)}$ and is thus more challenging to accurately describe. It is controlled by the Hessian of the loss:

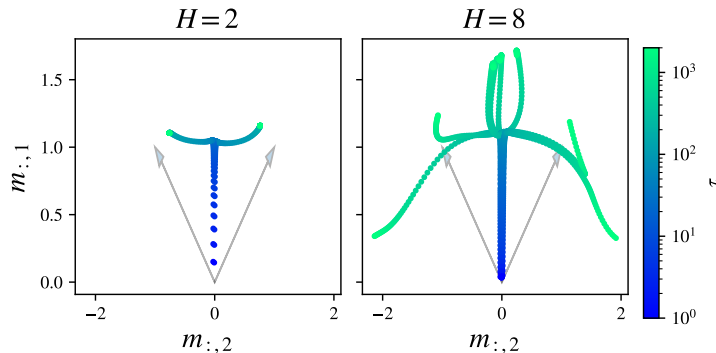


FIG. 2. Evolution of the H heads for the flipping spike distribution at $F = 2$, in the span of the “constant” direction k_1^* and the “flipping sign” direction k_2^* . σ softmax, $L = 4$, $\nu_1 = \nu_2 = 2$ and $\eta = 1$.

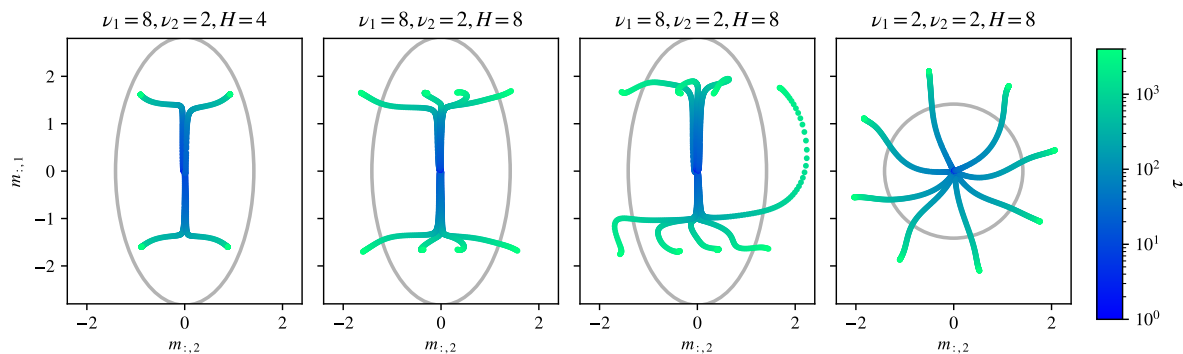


FIG. 3. Evolution of the heads for the non-isotropic Gaussian distribution at $F = 2$. σ softmax, $L = 4$, $\eta = 1$. The two central panels at $H = 8$ correspond to two different runs with different realizations of the initial condition.

the more negatively curbed the faster it is to escape the saddle in a direction. We state the following lemma on the structure of the Hessian before the specialization time τ^s , when the attention is not yet specialized, and after the time τ^u , so b and v for the softmax-1 reached their unspecialized minimum. This lemma is a simplification of the more detailed Lemma A.5 given and proven in Appendix A 2 b. We assume that $\|\mathbb{E}\theta\|_2$ and η are small enough so we can expand the loss around $m \approx 0$ and at $r = 0$.

Lemma III.1 (Hessian before specialization). *Consider $m \in \mathbb{R}^{H \times F}$ orthogonal to $\mathbb{E}\theta$ i.e. $m\mathbb{E}\theta = 0$. Assume that b is not specialized, and for the softmax-1 assume that b and v reached the fixed-point described by Lemma A.4. The loss can be expanded in m as the quadratic form*

$$\tilde{\mathcal{E}}_\sigma(m, 0, b, v) = \tilde{\mathcal{E}}_\sigma(0, 0, b, v) + \left(\mathbf{1}_H \mathbf{1}_H^\top \otimes (c_1^{(2)} I_F + (c_2^{(2)} + c_4^{(2)}) \text{Cov} \theta) - (c_3^{(2)} + c_4^{(2)}) I_H \otimes \text{Cov} \theta \right) \cdot (m, m) + \mathcal{O}(\|m\|_F^4) \quad (13)$$

with \otimes the tensorial product between the spaces \mathbb{R}^H and \mathbb{R}^F , and $c_1^{(2)}, c_2^{(2)}, c_3^{(2)} \in \mathbb{R}$ strictly positive and $c_4^{(2)} \in \mathbb{R}$ positive for all $L \geq 3$.

This lemma highlights a main phenomenon that occurs during specialization. Assuming that $\text{Cov} \theta$ is diagonal, the heads learn the features f sequentially, from the ones with the largest signal $\text{Var} \theta_f$ to the ones with smaller signal. This happens because the directions with larger $\text{Var} \theta_f$ have smaller negative eigenvalues. This makes a key connection with what [2, 3] observe in practice, where the attention first learn easy tasks such that bigram statistics and then harder such that n-grams and induction. This sequential learning is shown for the non-isotropic Gaussian distribution, where $\mathbb{E}\theta = 0$ and all the features f have different signal strengths in Figs. 3 and 4, as well as in Appendix Figs. 10 and 16 to 20. Notice that in the case where two features have the same signal strength, they are learned at the same time, as shown in Fig. 3 right. Lemma III.1 also shows that the heads tend to split orthogonally to $\mathbf{1}_H$, because this

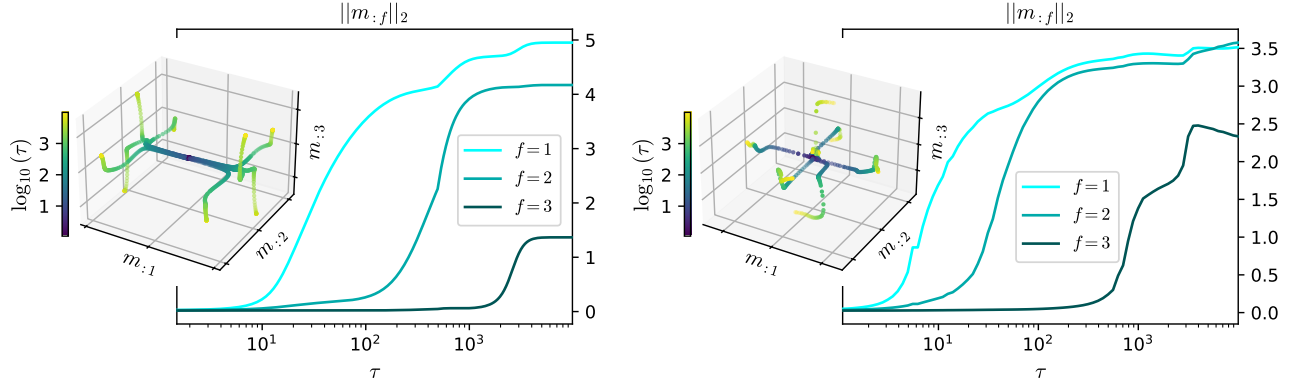


FIG. 4. Evolution of the $H = 8$ heads for the non-isotropic Gaussian distribution at $F = 3$, according to Prop. III.2. Left: σ softmax; right: σ B-softmax. $L = 5$, $\nu_1 = 20$, $\nu_2 = 1$ and $\eta = 1$.

direction is associated to a higher eigenvalue and thus avoided. The heads specialize into two even groups spanning the two signs of each direction.

Whenever $\text{Cov } \theta$ is not diagonal, the same reasoning holds in its eigenbasis. The heads perform principal component analysis (PCA) of θ , learning the eigenvectors $\{s_f \in \mathbb{R}^F\}_{f \in [F]}$ of $\text{Cov } \theta$ sequentially from higher to lower eigenvalue, as already observed by [8] for linear attention on in-context linear regression. However, a main difference with this work is that in our model each head does not focus on one eigenvector; instead, they can learn different combinations of $\{s_f\}_f$, as we detail in the next paragraphs.

B. Hierarchical specialization

Around the specialization time τ^s the attention starts learning the different features at different times. As soon as the first features are learnt, they influence the learning of the remaining features. We describe this interaction in the next lemma for the softmax, proven in Appendix A 2 b result A.6. We consider a feature f that is not yet learnt, i.e. $m_{:f} = 0$, while n features $\bar{f}_1, \dots, \bar{f}_n$ are already partially learnt. Because of Lemma III.1, we assume that $m_{:f}$ grows orthogonally to $\mathbf{1}_H$ and we restrict the analysis to this space.

Lemma III.2 (Hessian during specialization). *Take σ softmax. Assume that $\mathbb{E}\theta = 0$ and that the θ_f are independent. Let n be an integer, $\bar{f}_1, \dots, \bar{f}_n \in [F]^n$ all different, $\bar{m} \in \mathbb{R}^{H \times F}$ and assume that $\bar{m}_{:f} = 0$ for all $f \notin \{\bar{f}_1, \dots, \bar{f}_n\}$. Pick $f \notin \{\bar{f}_1, \dots, \bar{f}_n\}$; then the Hessian of the loss is*

$$\begin{aligned} \nabla_{m_{:f}, m_{:f}}^2 \tilde{\mathcal{E}}(\bar{m}, 0, 0, 0) &= \nabla_{m_{:f}, m_{:f}}^2 \tilde{\mathcal{E}}(0, 0) + \sum_i^n c_{1,i}^{(4)} \|\bar{m}_{:\bar{f}_i}\|_2^2 I_H \\ &+ \sum_i^n c_{2,i}^{(4)} \text{Diag}(\bar{m}_{:\bar{f}_i} \odot^2) + \sum_i^n c_{3,i}^{(4)} \bar{m}_{:\bar{f}_i} \bar{m}_{:\bar{f}_i}^\top + M + \mathcal{O}(\|\bar{m}\|_F^4) \end{aligned} \quad (14)$$

where M is a quadratic form that cancels when $m_{:f}^\top \mathbf{1}_H = 0$ and $\bar{m}^\top \mathbf{1}_H = 0$, and where $c_{1,i}^{(4)} > 0$, $c_{2,i}^{(4)} \in \mathbb{R}$, $c_{3,i}^{(4)} > 0$ for all $L \geq 3$ do not depend on \bar{m} .

This lemma gives the following insight into the dynamics of the heads. For a feature f that is not yet learnt, $m_{:f}$ tends to grow orthogonally to the magnetizations of each already-learnt feature $m_{:\bar{f}_i}$, because of the term $m_{:\bar{f}_i} m_{:\bar{f}_i}^\top$ associated to a more positive eigenvalue of the Hessian. Several patterns can emerge from this dynamics, depending on the activation function σ . The following observations rely on the numerical integration of the gradient descent.

For the softmax and the softmax-1, we observe that the different heads learn a full hierarchical representation of data: for each singular direction s_f , the heads split evenly in the two signs of the direction $\pm s_f$; and, if H is large enough, the heads learn all the 2^F binary combinations $\pm s_1 \pm s_2 \dots \pm s_F$. This is shown on Fig. 3 at $F = 2$ and $H = 4$ and in the inset of Fig. 4 at $F = 3$ and $H = 8$, as well as in Appendix Figs. 16 to 20. A similar hierarchical learning is described in [24] for deep linear fully-connected neural networks; yet notice that, contrary to this work, we do not impose any strong structure on the data P_θ since we only require anisotropy. Rather, the hierarchical learning comes from the structure of the multi-head attention itself.

The behaviour of the Bayes-softmax is different: each pair of heads tend to learn a single singular direction $\pm s_f$, as shown in Fig. 4 right. The fact that the heads learn orthogonal representations is specific to the distribution we consider in Fig. 4, and may not happen in other cases, as highlighted by Prop. IV.2 in the next part.

Later dynamics, excursions. The final split of the heads depends on the details of the initialization and on the global properties of the loss landscape, and hence is hard to characterize analytically. As can be seen in Fig. 3 at $H = 8$, because of the stochasticity in initialization, at the beginning of the learning the heads may not split evenly along a direction f , even if $P_\theta(\theta_f)$ is symmetric in this direction. However, later in the learning, the misplaced heads can rearrange, by performing an *excursion*, so that at the end the split is even and the loss optimized. This shows that the structure of the multi-head softmax helps SGD to navigate in the loss landscape and not to stay stuck in bad local minima.

IV. HEAD DEACTIVATION VIA ALTERNATIVE ACTIVATION

In this section, we consider the trained models and the achieved loss $\mathcal{E}_\sigma^\infty = \lim_{\tau \rightarrow \infty} \mathcal{E}_\sigma(k(\tau), b(\tau), v(\tau))$, for different activations σ . We start by deriving the Bayes risk on our probabilistic data model, motivating the Bayes-softmax attention; we compare the expressivity and the performances of the other activations functions and we highlight the impact of the normalization of the heads.

A natural benchmark is the Bayes risk $\mathcal{E}_{\text{Bayes}} = \mathbb{E}_{k^*, X, y} \|y - \hat{y}_{\text{Bayes}}(X, k^*)\|_2^2$. It corresponds to the loss of the Bayes estimator \hat{y}_{Bayes} , which is the optimal estimator of y in terms of population loss. We characterize it in the following proposition and derive it in Appendix A 3.

Proposition IV.1 (Bayes estimator). *Given the spikes $\{k_f^*\}_{f \in [F]} \in \mathbb{R}^{F \times D}$ and a sequence $X \in \mathbb{R}^{L \times D}$, the Bayes estimator of the label is*

$$\hat{y}_{\text{Bayes}}(X, k^*) = \sum_{\ell}^L P(\epsilon = \ell | X, k^*) X_{\ell} \quad (15)$$

$$P(\epsilon = \ell | X, k^*) = \frac{\int_{\theta} \exp(\hat{k}(\theta)^T X_{\ell}) e^{-\frac{\|\theta\|_2^2}{2}} P_{\theta}(d\theta)}{\sum_{\ell'}^L \int_{\theta} \exp(\hat{k}(\theta)^T X_{\ell'}) e^{-\frac{\|\theta\|_2^2}{2}} P_{\theta}(d\theta)} \quad (16)$$

with $\hat{k}(\theta) = \sum_f^F \theta_f k_f^*$.

In practice, one does not have access to the spikes k^* nor to P_{θ} , and \hat{y}_{Bayes} seems to be a purely theoretical estimator. Yet, k^* and P_{θ} can be learned and \hat{y}_{Bayes} can be interpreted as the Bayes-softmax attention, which we rewrite as

$$\hat{y}_{\text{B-softmax}, k, b}(X) = \sum_{\ell}^L \frac{\sum_h^H \exp(k_h^{\top} X_{\ell} + b_h)}{\sum_{\ell'}^L \sum_{h'}^H \exp(k_{h'}^{\top} X_{\ell'} + b_{h'})} X_{\ell} . \quad (17)$$

We state the equivalence between the Bayes estimator and the Bayes-softmax attention in the following proposition, which directly follows from a substitution of the given parameters into the B-softmax attention model leading to the expression of the Bayes estimator Prop. IV.1.

Proposition IV.2 (Optimality of the Bayes-softmax attention). *Consider some distribution P_{θ} with discrete support $\{\theta^h\}_{h \in [H]}$. Then the Bayes-softmax attention with H heads and parameters $k_h = \hat{k}(\theta^h)$ and $b_h = -\|\theta^h\|_2^2 \log P_{\theta}(\theta^h)/2$ achieves the Bayes risk.*

This proposition gives a prescription on the right number H of attention heads: each point of the support of P_{θ} should correspond to a different attention head. This can be generalised to continuous distribution P_{θ} by discretizing the integral in Prop. IV.1 and taking H large enough to approximate it correctly. In Fig. 5 we can see that when the distribution of the spikes is discrete, the loss of the B-softmax model reaches a plateau to the Bayes risk when the number of heads is greater than or equal to the number of spikes. This shows that the B-softmax trained with SGD can exactly estimate the hidden parameters of the Bayes-risk and reach the optimality, whenever H is large enough. For a continuous distribution, the loss does not plateau and continues to decrease, and more heads are required to interpolate P_{θ} and approach the Bayes-risk. The same behaviour qualitatively holds for the softmax and the softmax-1, though the equivalence with the Bayes risk does not hold.

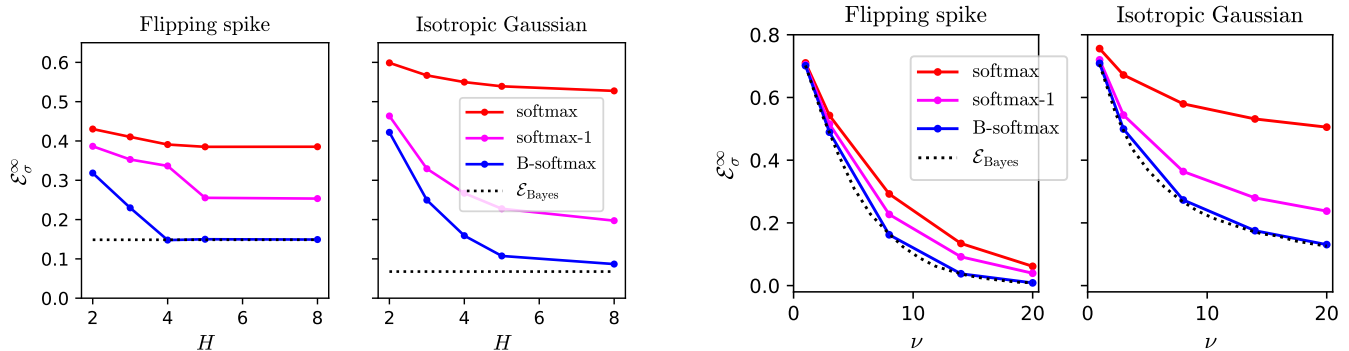


FIG. 5. Predicted error $\mathcal{E}_\sigma^\infty$ of the different activation functions after training. $L = 5$, $\eta = 1$. Left: $F = 4$, $\nu = 10$, varying H ; right: $F = 2$, $H = 4$, varying signal strength. We performed 5 runs with different initial conditions; the standard deviations are not visible.

The most noticeable property of the Bayes-softmax activation is its ability to deactivate some of the heads via normalization. In our setting, heads that are not aligned with the signal \hat{k} introduce noise that cannot be reduced by other means. This misalignment has to be mitigated by the architecture of the attention itself, by “switching off” the heads with low attention scores. However, this ability is not unique to B-softmax activation. While the standard softmax is not able to do so and therefore cannot reach zero error, the softmax-1 can deactivate heads and outperform the standard variant, as stated by the following result derived in Appendix A 3.

Proposition IV.3 (Expressivity of softmax and softmax-1). *Assume that P_θ is not restricted to a half-space of \mathbb{R}^F , i.e. there is some disjoint $S \subset \mathbb{R}^F$ and $\bar{S} = \{-\theta, \theta \in S\}$ such that $P_\theta(S)$ and $P_\theta(\bar{S})$ are bounded away from zero by some constant. Then the softmax attention is not well specified, i.e. $\mathcal{E}_{\text{softmax}}(k, 0, 0)$ is bounded away from zero for all k .*

Consider the attention equipped with the softmax-1 activation function. Assume that $\|\theta\|_2 > B$ almost surely. Then in limit of large signal $B \rightarrow \infty$ (taken after $D \rightarrow \infty$) the softmax-1 attention is well specified, i.e. there is k , b and v such that $\mathcal{E}_{\text{softmax-1}}(k, b, v) \rightarrow 0$.

Prop. IV.3 is illustrated by Fig. 5. For the flipping sign direction, the signal \hat{k} is restricted to a quadrant of \mathbb{R}^F and therefore all the heads of the softmax can be positively aligned with it; the softmax and the softmax-1 have close performances for all signal strengths. This has to be contrasted with the isotropic Gaussian distribution, where the heads cannot always be aligned with \hat{k} : the gap between softmax and softmax-1 increases with the signal strength ν , and the softmax plateaus at large ν . In the two cases, the B-softmax is very close to the Bayes risk and achieve better performances, as expected. Independent of its link with the Bayes estimator, the superiority of the B-softmax over the softmax-1 can be explained by its ability to perform an in-context normalization. For the B-softmax, the normalization of each head depends on all the other heads and can adapt to a particular sequence, while for the softmax-1 the normalization is done by the coefficients e^{b_h} that are fixed and that let the heads interact only during training.

The attention maps of the different attentions are shown in Fig. 6 for a few sequences drawn from the isotropic Gaussian distribution. The attention map of the softmax is noisy: the heads that do not focus on the relevant token have to focus on irrelevant ones, while the softmax-1 reduces attention scores of the “irrelevant” heads, and this effect is even more prominent for the B-softmax.

The softmax-1 and B-softmax rely on the multiple heads in a more optimal and specialized way. To see this, we perform a head pruning experiment and compare the importance of the heads. The pruning of the trained heads is done in a greedy manner and we uniformly rescale the output to keep constant the amplitude of the attention scores. The results of the experiment are reported on Fig. 7. Similarly to previous empirical studies [6, 7], we observe that a substantial number of heads can be removed without seriously affecting performance. In our model, in the case of a flipping spike distribution over F spikes or an isotropic Gaussian in dimension F , the number of heads \tilde{H} that can be pruned without significant loss of performance is close to $H - F$; i.e. we can keep one head per each hidden feature approximatively. If one prunes more heads $\tilde{H} > H - F$ and removes the heads that are actually necessary for the inference, the softmax-1 and the B-softmax behave differently from the standard softmax. Their performances degrade more severely than softmax and with a larger variance over the repeated runs. This suggests that attention with softmax-1 or B-softmax activation strongly relies on all the necessary heads together, and that these are strongly specialized.

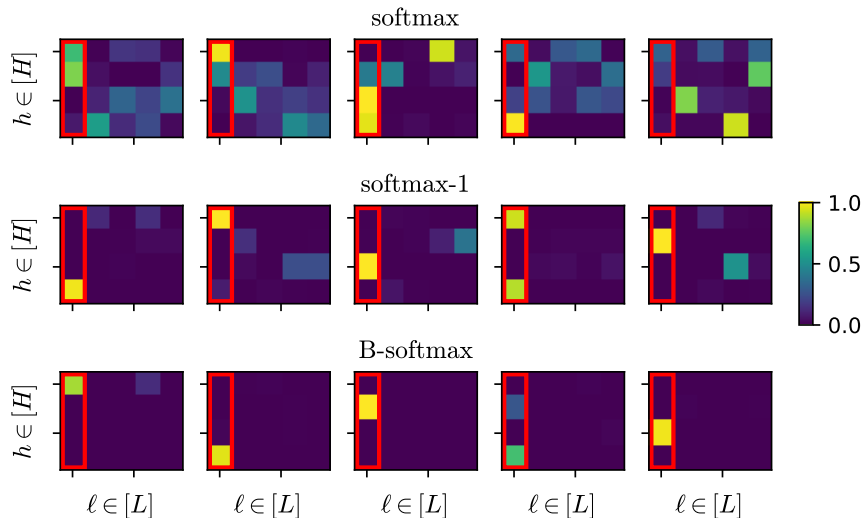


FIG. 6. Attention maps of the different activation functions after training. $H = 4$ heads, $L = 5$ and the relevant token is highlighted in the red rectangle. We show the attention maps for five independent sequences. $F = 3$, signal isotropic Gaussian of strength $\nu = 9$.

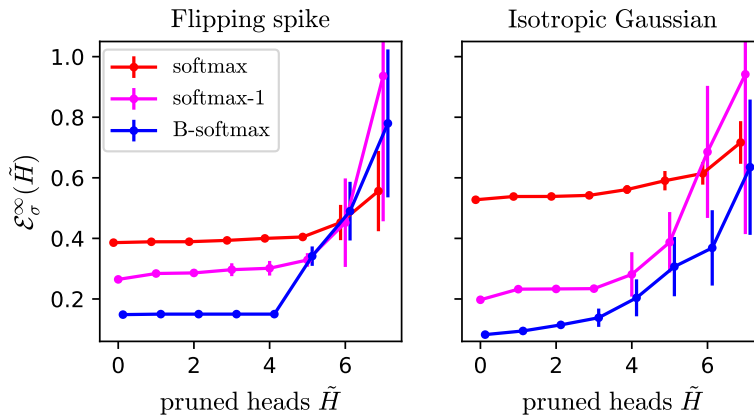


FIG. 7. Pruning head experiment. Error $\mathcal{E}_\sigma^\infty(\tilde{H})$ of the different activation functions after training, after pruning \tilde{H} heads over $H = 8$ total heads. $L = 5$, $F = 4$, $\nu = 10$. We performed five training runs with different initial conditions.

V. CONCLUSION

We introduced a solvable high-dimensional model of multi-head attention that isolates staged head specialization, head redundancy, and the role of attention normalization under SGD training. By restricting to a minimal architecture, we obtained an exact description of training dynamics and identified regimes where redundant heads induce persistent variance unless explicitly suppressed by the activation.

Our model is intentionally simplified. It considers a single attention layer, excludes output projections and residual pathways, and focuses on a stylized sequence-to-token regression task. Extending the analysis to deeper architectures and more structured data distributions remains an open direction. As in the theory of the multi-index model [14], the population-level training dynamics derived here are expected to translate into sharp sample-complexity transitions under empirical risk minimization, suggesting a route toward understanding data-dependent phase transitions in attention-based models.

Finally, comparing the overall phenomenology discovered in our model with recent works on in-context learning [8, 9], we see that stagewise head emergence appears in both settings. By contrast, the effect of head redundancy is model-dependent: in our setting, redundant heads induce persistent variance unless suppressed by the attention normalization, while in ICL regression, redundant components are asymptotically harmless.

ACKNOWLEDGMENT

We thank Ludovic Stephan, as well as Pierre Marion and Claire Boyer for discussion about the single location models.

We acknowledge funding from the Swiss National Science Foundation grants SNSF SMARtNet (grant number 212049), and the Simons Collaboration on the Physics of Learning and Neural Computation via the Simons Foundation grant (#1257413 (LZ)).

-
- [1] K. Clark, U. Khandelwal, O. Levy, and C. D. Manning, What does bert look at? an analysis of bert’s attention, arXiv preprint arXiv:1906.04341 (2019).
- [2] J. Hoogland, G. Wang, M. Farrugia-Roberts, L. Carroll, S. Wei, and D. Murfet, Loss landscape degeneracy and stagewise development in transformers, *Transactions on Machine Learning Research (TMLR)* (2024), arxiv:2402.02364.
- [3] G. Wang, J. Hoogland, S. van Wingerden, Z. Furman, and D. Murfet, Differentiation and specialization of attention heads via the refined local learning coefficient, in *International Conference on Learning Representations (ICLR)* (2025) arXiv:2410.02984.
- [4] A. Chen, R. Shwartz-Ziv, K. Cho, M. L. Leavitt, and N. Saphra, Sudden drops in the loss: Syntax acquisition, phase transitions, and simplicity bias in mlms, in *International Conference on Learning Representations (ICLR)* (2024) arXiv:2309.07311.
- [5] C. Tigges, M. Hanna, Q. Yu, and S. Biderman, Llm circuit analyses are consistent across training and scale, in *Advances in Neural Information Processing Systems (NeurIPS)* (2024) arXiv:2407.10827.
- [6] P. Michel, O. Levy, and G. Neubig, Are sixteen heads really better than one?, in *Advances in Neural Information Processing Systems (NeurIPS)*, Vol. 32 (Curran Associates, Inc., 2019) arXiv:1905.10650.
- [7] E. Voita, D. Talbot, F. Moiseev, R. Sennrich, and I. Titov, Analyzing multi-head self-attention: Specialized heads do the heavy lifting, the rest can be pruned, in *Proceedings of the 57th Annual Meeting of the Association for Computational Linguistics* (Association for Computational Linguistics, 2019) arXiv:1905.09418.
- [8] Y. Zhang, A. K. Singh, P. E. Latham, and A. Saxe, Training dynamics of in-context learning in linear attention, in *Proceedings of the 42th International Conference on Machine Learning (ICML)* (2025) arXiv:2501.16265.
- [9] S. Chen, H. Sheen, T. Wang, and Z. Yang, Training dynamics of multi-head softmax attention for in-context learning: Emergence, convergence, and optimality, in *Conference on Learning Theory (COLT)* (2024) arXiv:2402.19442.
- [10] H. S. Seung, H. Sompolinsky, and N. Tishby, Statistical mechanics of learning from examples, *Physical review A* **45**, 6056 (1992).
- [11] D. Saad and S. Solla, Dynamics of on-line gradient descent learning for multilayer neural networks, *Advances in neural information processing systems* **8** (1995).
- [12] D. Saad, S. A. Solla, *et al.*, On-line learning in soft committee machines, *Physical review E* **52**, 4225 (1995).
- [13] A. Engel, *Statistical mechanics of learning* (Cambridge University Press, 2001).
- [14] B. Aubin, A. Maillard, F. Krzakala, N. Macris, L. Zdeborová, *et al.*, The committee machine: Computational to statistical gaps in learning a two-layers neural network, *Advances in Neural Information Processing Systems* **31** (2018).
- [15] S. Goldt, M. Advani, A. M. Saxe, F. Krzakala, and L. Zdeborová, Dynamics of stochastic gradient descent for two-layer neural networks in the teacher-student setup, *Advances in neural information processing systems* **32** (2019).
- [16] G. Ben Arous, R. Gheissari, and A. Jagannath, Online stochastic gradient descent on non-convex losses from high-dimensional inference, *Journal of Machine Learning Research (JMLR)* **22**, 1 (2021).
- [17] E. Abbe, E. B. Adserà, and T. Misiakiewicz, Sgd learning on neural networks: leap complexity and saddle-to-saddle dynamics, in *Proceedings of the 36th International Conference on Machine Learning (ICML)* (2023) arXiv:2302.11055.
- [18] L. Arnaboldi, B. Loureiro, L. Stephan, F. Krzakala, and L. Zdeborová, Asymptotics of SGD in sequence-single index models and single-layer attention networks, in *Advances in Neural Information Processing Systems (NeurIPS)* (2025) arXiv:2506.02651.
- [19] P. Marion, R. Berthier, G. Biau, and C. Boyer, Attention layers provably solve single-location regression, in *The Thirteenth International Conference on Learning Representations (ICLR)* (2025) arXiv:2410.01537.
- [20] E. Troiani, H. Cui, Y. Dandi, F. Krzakala, and L. Zdeborová, Fundamental limits of learning in sequence multi-index models and deep attention networks: High-dimensional asymptotics and sharp thresholds, *Forty-second International Conference on Machine Learning (ICML)* (2025).
- [21] O. Duranthon, P. Marion, C. Boyer, B. Loureiro, and L. Zdeborová, Statistical advantage of softmax attention: Insights from single-location regression, in *The Fourteenth International Conference on Learning Representations (ICLR)* (2026) arXiv:2509.21936.
- [22] N. Barnfield, H. Cui, and Y. M. Lu, High-dimensional analysis of single-layer attention for sparse-token classification (2025), arXiv:2509.25153.
- [23] E. Dohmatob, Understanding softmax attention layers: Exact mean-field analysis on a toy problem, in *Advances in Neural Information Processing Systems (NeurIPS)* (2025).
- [24] A. M. Saxe, J. L. McClelland, and S. Ganguli, A mathematical theory of semantic development in deep neural networks, *PNAS* **116** (2019), arxiv:1810.10531.

- [25] P. Kaul, C. Ma, I. Elezi, and J. Deng, From attention to activation: Unraveling the enigmas of large language models, in *International Conference on Learning Representations (ICLR)*, Vol. 2025 (2025) pp. 34531–34582, arXiv:2410.17174.
- [26] T. Darcet, M. Oquab, J. Mairal, and P. Bojanowski, Vision transformers need registers, in *International Conference on Learning Representations (ICLR)* (2024) arXiv:2309.16588.
- [27] G. Xiao, Y. Tian, B. Chen, S. Han, and M. Lewis, Efficient streaming language models with attention sinks, in *International Conference on Learning Representations (ICLR)* (2024) arXiv:2309.17453.
- [28] Z. Qiu, Z. Wang, B. Zheng, Z. Huang, K. Wen, S. Yang, R. Men, L. Yu, F. Huang, S. Huang, D. Liu, J. Zhou, and J. Lin, Gated attention for large language models: Non-linearity, sparsity, and attention-sink-free, in *The Thirty-ninth Annual Conference on Neural Information Processing Systems (NeurIPS)* (2025) arXiv:2505.06708.
- [29] N. Carion, F. Massa, G. Synnaeve, N. Usunier, A. Kirillov, and S. Zagoruyko, End-to-end object detection with transformers, in *Computer Vision – ECCV 2020* (Springer International Publishing, 2020) pp. 213–229, arXiv:2005.12872.
- [30] L. Arnaboldi, Y. Dandi, F. Krzakala, B. Loureiro, L. Pesce, and L. Stephan, Online learning and information exponents: On the importance of batch size, and time/complexity tradeoffs, arXiv preprint arXiv:2406.02157 (2024).

Appendix A: Proofs of propositions and lemma.

In this part we give the different proofs and justifications for our theoretical results of parts III and IV.

1. Low-dimensional characterization of SGD

We start by deriving the asymptotic characterization of the training dynamics in terms of the order parameters.

Proof of Proposition III.1. We first derive the order parameters and the expression for the reparameterized loss. Notice that in the high-dimensional limit when $D \rightarrow \infty$, the hidden spikes directions k_f^* are almost orthogonal. Then parameters of the attention model k_1, \dots, k_H can be expressed as follows:

$$k_h = \sum_{f=1}^F m_{hf} k_f^* + \sum_{h'=1}^H r_{hh'} k_{h'}^\perp,$$

where $\{k_{h'}^\perp\}_{h' \in [H]}$ are vectors orthogonal to $\{k_f^*\}_{f \in [F]}$ and between each other, and

$$m_{hf} = (k_h)^\top k_f^*, \quad h \in [H], f \in [F] \quad q_{hh'} = (k_h)^\top k_{h'}, \quad h, h' \in [H] \quad (\text{A1})$$

$$p_{ff'} = (k_f^*)^\top k_{f'}^* \approx \delta_{f,f'}, \quad f, f' \in [F] \quad r = (q - mp^{-1}m^\top)^{1/2} \quad (\text{A2})$$

Thus, the pre-activations χ_h of the attention head h can be expressed as

$$\chi_h = \sum_{f=1}^F m_{hf} X k_f^* + \sum_{h'=1}^H r_{hh'} X k_{h'}^\perp,$$

or, if we denote $\chi_f^* = X k_f^*$ and $\xi_{h'} = X k_{h'}^\perp$

$$\chi_h = \sum_{f=1}^F m_{hf} \chi_f^* + \sum_{h'=1}^H r_{hh'} \xi_{h'}. \quad (\text{A3})$$

The risk depends on the parameters only via the projections χ_h , and in the high-dimensional limit the projections χ_f^* and $\xi_{h'}$ are normally distributed, such that all elements of the vectors are independent, $\chi_{f\ell}^* \sim \mathcal{N}(\delta_{\ell, \epsilon^*} \theta_f, 1)$, and $\xi_{h'\ell} \sim \mathcal{N}(0, 1)$.

We can now express the loss in terms of the order parameters. We begin by explicitly writing the output of the attention model and expanding the norm squared:

$$\mathcal{E}_\sigma(k, b, v) = \frac{1}{D} \mathbb{E}_{\epsilon, \theta, X} \left[\|X_\epsilon\|_2^2 - \frac{2}{H} \sum_{h=1}^H \sigma(\chi, b, v; h)^T X X_\epsilon + \frac{1}{H^2} \sum_{h=1}^H \sum_{h'=1}^H \sigma(\chi, b, v; h)^T X X^T \sigma(\chi, b, v; h') \right].$$

This can be simplified using independence of the tokens X_ℓ and noticing that $\mathbb{E}_X \|X_\ell\|_2^2 \rightarrow D$ when $D \rightarrow \infty$.

$$\begin{aligned} \mathcal{E}_\sigma(k, b, v) &= \frac{1}{D} \mathbb{E}_{\epsilon, \theta, X} \left[\|X_\epsilon\|_2^2 - \frac{2}{H} \sum_{h=1}^H \sigma(\chi, b, v; h)_\epsilon \|X_\epsilon\|_2^2 + \frac{1}{H^2} \sum_{h=1}^H \sum_{h'=1}^H \sum_{\ell=1}^L \sigma(\chi, b, v; h)_\ell \sigma(\chi, b, v; h')_\ell \|X_\ell\|_2^2 \right] \\ &= \frac{1}{D} \mathbb{E}_{\epsilon, \theta, X} \sum_{\ell=1}^L \|X_\ell\|_2^2 \left(\delta_{\ell, \epsilon} - \frac{1}{H} \sum_{h=1}^H \sigma(\chi, b, v; h)_\ell \right)^2 = \mathbb{E}_{\epsilon, \theta, X} \sum_{\ell=1}^L \left(\delta_{\ell, \epsilon} - \frac{1}{H} \sum_{h=1}^H \sigma(\chi, b, v; h)_\ell \right)^2. \end{aligned}$$

Using the expression (A3), we get the final expression for $\tilde{\mathcal{E}}$. □

2. Description of the dynamics

a. The two dynamical phases

We justify the description of the dynamics in the two phases Props. III.3 and III.4. We give a sketch of a proof; a more formal derivation would follow [16–18, 30]. We rely on several lemma about the gradient and the hessian of the loss $\tilde{\mathcal{E}}$ in the space of the order parameters. These lemma are stated and proved in part A 2 b.

a. Unspecialized phase Prop. III.3. Assuming $\mathbb{E}\theta \neq 0$, according to Lemma A.1 and A.2, the space \mathcal{M}_u of unspecialized m , r and b is invariant by the gradient flow; and moreover the subspace of m proportional to $\mathbf{1}_H(\mathbb{E}\theta)^\top$ is also invariant by the gradient flow. At initialization $m \approx 0$, $r \approx I_H$, $b = 0$ are unspecialized; and the gradient of the loss w.r.t. m does not vanish and points towards $\mathbf{1}_H(\mathbb{E}\theta)^\top$. Consequently only a few time steps τ^u are necessary to move in this direction, i.e. a time $\tau^u = \Theta(1)$ is enough so that $m = x\mathbf{1}_H(\mathbb{E}\theta)^\top$ with $x = \Theta(1) \in \mathbb{R}^+$. The total number of required samples is $N = tN_b = \tau^u \gamma^{-1} N_b = \omega(D)$.

As to b and v , for the softmax-1, according to Lemma A.4, the gradient at initialization does not vanish and points towards unspecialized fixed-points that are reached in time $\tau = \Theta(1)$. For the B-softmax the gradient w.r.t. b at initialization is null, b does not move and stays unspecialized.

Because of finite sizes, m and r are not exactly initialized on \mathcal{M}_u . There is an error of order $\Theta(D^{-1/2})$ that requires a time $\tau^s = \Theta(\log D)$ to grow. Consequently the dynamics stays in the unspecialized space until this specialization time τ^s .

b. Specialization phase Prop. III.4. We rely on Lemma III.1 on the Hessian of the loss at small m and r and unspecialized b . This lemma applies even after initialization, as we justify by the following assumptions.

We assume that $\|\mathbb{E}\theta\|_2$ is small enough so during the unspecialized phase the growth of m remains bounded and we can consider the loss at $m \approx 0$. We moreover consider a small enough initialization η so $r \approx 0$. By Lemma A.3 on the gradient, $r = 0$ is a fixed-point of the dynamics, and by Lemma III.1 on the Hessian it is a stable fixed-point for m small enough. Consequently $r \approx 0$ holds even after initialization, until m starts growing during the specialization phase. Numerically, we observe that $r = 0$ is a stable fixed-point whose bassin of attraction encompasses values of m and r of order one. Last, b stays unspecialized until m grows and specializes, because it corresponds to a stable or flat point by Lemma III.1.

Lemma III.1 gives that there exists directions orthogonal to $\mathbb{E}\theta$ in the space of the features, that are descent directions and where the Hessian is not degenerated. More precisely, assuming the heads split evenly and that $m^\top \mathbf{1}_H \approx 0$, the descent directions are the eigenvectors of $\text{Cov}\theta$ projected in the orthogonal space, and the Hessian has stricly negative eigenvalues in all these directions. Consequently m escapes the saddle exponentially fast in τ , i.e. there is some independent of D positive operator C such that $m(\tau) = \exp(\tau C)m(0)$. Since at random initialization $m = \Theta(D^{-1/2})$, it requires a time $\tau^s = \Theta(\log D)$ to start moving in the orthogonal space. The total number of required samples is $N = \tau^s \gamma^{-1} N_b = \omega(D \log D)$.

The heads specialize because they tend to evolve orthogonally to $\mathbf{1}_H$. In the space where $m^\top \mathbf{1}_H \neq 0$ the Hessian has stricly larger eigenvalues and thus it requires more time to move in this direction.

b. Derivatives of the loss

We derive the technical results about the gradient, the hessian and the 4th order derivative of the loss $\tilde{\mathcal{E}}$ in the space of the order parameters. For the derivative of the activation function we use the notation

$$\partial_{h'\ell'} \sigma(\chi, b, v; h)_\ell = \frac{\partial}{\partial \chi_{h'\ell'}} \sigma(\chi, b, v; h)_\ell. \quad (\text{A4})$$

Lemma A.1 (Invariance of the unspecialized manifold by gradient descent.). *Consider the unspecialized manifold \mathcal{M}_u , where the heads are not specialized, defined by $m = \mathbf{1}_H \tilde{m}^\top$ with $\tilde{m} \in \mathbb{R}^F$, $r = \tilde{r}_1 I_H + \tilde{r}_2 \mathbf{1}_H \mathbf{1}_H^\top$ with $\tilde{r}_1 > 0$, $\tilde{r}_1 + H\tilde{r}_2 > 0$ and $b = \tilde{b} \mathbf{1}_H$ with $\tilde{b} \in \mathbb{R}$. \mathcal{M}_u is invariant by the gradient descent eq. (12).*

Proof. The loss is invariant by permutation of the heads and therefore on \mathcal{M}_u $\nabla_{m_h} \tilde{\mathcal{E}}_\sigma$, $\partial_{r_{hh}} \tilde{\mathcal{E}}_\sigma$, $\partial_{r_{h \neq h'}} \tilde{\mathcal{E}}_\sigma$ and $\partial_{b_h} \tilde{\mathcal{E}}_\sigma$ do not depend on h . \square

Lemma A.2 (Gradient of the loss at initialization and in the unspecialized phase). *Let $\mathbb{E}\theta = (\mathbb{E}_{P_\theta} \theta_f)_{f \in [F]} \in \mathbb{R}^F$ be the mean of the signal. Take m , r and b on the unspecialized manifold \mathcal{M}_u . Take all the heads aligned with $\mathbb{E}\theta$, i.e. take $x \in \mathbb{R}$ and $m_h = x\mathbb{E}\theta$ for all h . There is $c^{(1)}(x, r, b, v) \in \mathbb{R}$ such that for all h*

$$\nabla_{m_h} \tilde{\mathcal{E}}_\sigma(m, r, b, v) = -c^{(1)}(x, r, b, v)\mathbb{E}\theta. \quad (\text{A5})$$

Moreover at initialization $c^{(1)}(0, r, 0, 1) > 0$.

Proof. We compute the gradient of the loss in the space of the order parameters. We remind that the reparameterized loss is

$$\tilde{\mathcal{E}}_\sigma(m, r, b, v) = \mathbb{E}_{\epsilon, \theta, \chi^*, \xi} \left[\sum_{\ell}^L \left(\delta_{\ell, \epsilon} - \frac{1}{H} \sum_{h'}^H \sigma(\chi, b, v; h')_{\ell} \right)^2 \right] \quad (\text{A6})$$

$$\chi_{h\ell} = \sum_f^F m_{hf} \chi_{f\ell}^* + \sum_{h'}^H r_{hh'} \xi_{h'} \quad , \quad h \in [H], \ell \in [L]. \quad (\text{A7})$$

with $\epsilon \sim \text{Unif}(\{1, \dots, L\})$, $\theta \sim P_\theta$ and conditionally on ϵ and θ , $\chi_{:, \ell}^* \sim \mathcal{N}(\delta_{\ell, \epsilon} \theta, I_F)$ and $\xi_{:, \ell} \sim \mathcal{N}(0, I_H)$ for $\ell \in [L]$. The gradient is

$$\nabla_{m_h} \tilde{\mathcal{E}}_\sigma(m, r, b, v) = 2\mathbb{E}_{\epsilon, \theta, \chi^*, \xi} \sum_{\ell}^L \left(\frac{1}{H} \sum_{h'}^H \sigma(\chi, b, v; h')_{\ell} - \delta_{\ell, \epsilon} \right) \sum_{h', \ell'}^{H, L} \partial_{h\ell'} \sigma(\chi, b, v; h')_{\ell} \chi_{:, \ell'}^*. \quad (\text{A8})$$

We show the gradient is colinear to $\mathbb{E}\theta$ if all heads align with $\mathbb{E}\theta$, i.e. $m_h = x\mathbb{E}\theta$ for all $h \in [H]$. Let $w \in \mathbb{R}^F$ be orthogonal to $\mathbb{E}\theta$.

$$w^\top \nabla_{m_h} \tilde{\mathcal{E}}_\sigma(m, r, b, v) = 2\mathbb{E}_{\epsilon, \theta, \chi, \xi} \sum_{\ell}^L \left(\frac{1}{H} \sum_{h'}^H \sigma(\chi, b, v; h')_{\ell} - \delta_{\ell, \epsilon} \right) \sum_{h', \ell'}^{H, L} \partial_{h\ell'} \sigma(\chi, b, v; h')_{\ell} w^\top \chi_{:, \ell'}^*. \quad (\text{A9})$$

Then by orthogonality $w^\top \chi_{:, \ell'}^*$ and $\chi_{h\ell} = x(\mathbb{E}\theta)^\top \chi_{:, \ell}^* + \dots$ are independent gaussian random variables for all ℓ, ℓ' . Thus, we can factorize the expectation. Since $\mathbb{E} w^\top \chi_{:, \ell'}^* = w^\top \mathbb{E}\theta = 0$, we have $w^\top \nabla_{m_h} \tilde{\mathcal{E}}_\sigma(m, r, b, v) = 0$. Moreover we consider the unspecialized manifold, and so there is a same $c^{(1)}(x, r, b, v) \in \mathbb{R}$ for all h such that $\nabla_{m_h} \tilde{\mathcal{E}}_\sigma(m, r, b, v) = -c^{(1)}(x, r, b, v)\mathbb{E}\theta$.

At initialization $b = 0$, $v = 1$ and $m = 0$, and we have $\chi_{h'}$ independent of $\{\chi_h^*\}_{h \in [H]}$ for all h' ; thus

$$\nabla_{m_h} \tilde{\mathcal{E}}_\sigma(0, r, 0, 1) = 2\mathbb{E}_{\epsilon, \xi} \sum_{\ell}^L \left(\frac{1}{H} \sum_{h'}^H \sigma(\chi, 0, 1; h')_{\ell} - \delta_{\ell, \epsilon} \right) \sum_{h', \ell'}^{H, L} \partial_{h\ell'} \sigma(\chi, 0, 1; h')_{\ell} \mathbb{E}_{\theta, \chi} \chi_{:, \ell'}^* \quad (\text{A10})$$

$$= 2\mathbb{E}_{\epsilon, \xi} \sum_{\ell}^L \left(\frac{1}{H} \sum_{h'}^H \sigma(\chi, 0, 1; h')_{\ell} - \delta_{\ell, \epsilon} \right) \sum_{h'}^H \partial_{h\epsilon} \sigma(\chi, 0, 1; h')_{\ell} \mathbb{E}\theta \quad (\text{A11})$$

$$= 2\mathbb{E}_{\epsilon, \xi} \left(\frac{1}{H} \sum_{h'}^H \sigma(\chi, 0, 1; h')_{\epsilon} - 1 \right) \sum_{h'}^H \partial_{h\epsilon} \sigma(\chi, 0, 1; h')_{\epsilon} \mathbb{E}\theta \quad (\text{A12})$$

$$+ 2\mathbb{E}_{\epsilon, \xi} \sum_{\ell \neq \epsilon}^L \frac{1}{H} \sum_{h'}^H \sigma(\chi, 0, 1; h')_{\ell} \sum_{h'}^H \partial_{h\epsilon} \sigma(\chi, 0, 1; h')_{\ell} \mathbb{E}\theta$$

The two pre-factors in front of $\mathbb{E}\theta$ are negative because

$$\frac{1}{H} \sum_{h'}^H \sigma(\chi, 0, 1; h')_{\epsilon} - 1 < 0 \quad \sum_{h'}^H \partial_{h\epsilon} \sigma(\chi, 0, 1; h')_{\epsilon} > 0 \quad (\text{A13})$$

$$\frac{1}{H} \sum_{h'}^H \sigma(\chi, 0, 1; h')_\ell > 0 \qquad \sum_{h'}^H \partial_{h\epsilon} \sigma(\chi, 0, 1; h')_\ell < 0 \quad (\text{A14})$$

for all $\epsilon \neq \ell$, h , χ and for the three different activation functions σ . Consequently $c^{(1)}(0, r, 0, 1) > 0$. \square

Lemma A.3 (Gradient of the loss with respect to r at small r). *Consider $r = 0$, then for all m*

$$\nabla_r \tilde{\mathcal{E}}_\sigma(m, 0, b, v) = 0. \quad (\text{A15})$$

Proof. The loss is a symmetric function of r : it is invariant by the change of variables $(r, \xi) \mapsto (-r, -\xi)$. Therefore its gradient is null at $r = 0$. \square

Lemma A.4 (Gradient of the loss with respect to b and v at small m and r for the softmax-1). *Consider $m = 0$, $r = 0$ and σ to be the softmax-1. Take unspecialized heads i.e. $b = \tilde{b} \mathbf{1}_H$ for $\tilde{b} \in \mathbb{R}$. Then*

$$\nabla_{\tilde{b}} \tilde{\mathcal{E}}_\sigma(0, 0, b, v) = -2 \left(\frac{Lv}{L + e^{\tilde{b}}} - 1 \right) \frac{v}{H} \frac{e^{\tilde{b}}}{(L + e^{\tilde{b}})^2} \quad (\text{A16})$$

$$\nabla_v \tilde{\mathcal{E}}_\sigma(0, 0, b, v) = 2 \left(\frac{Lv}{L + e^{\tilde{b}}} - 1 \right) \frac{1}{L + e^{\tilde{b}}} \quad (\text{A17})$$

The fixed-points of this system satisfy $Lv = L + e^{\tilde{b}}$ and they are attractive. Last at initialization $b = 0$ and $v = 1$ and

$$\nabla_{\tilde{b}} \tilde{\mathcal{E}}_\sigma(0, 0, 0, 1) > 0 \quad (\text{A18})$$

$$\nabla_v \tilde{\mathcal{E}}_\sigma(0, 0, 0, 1) < 0 \quad (\text{A19})$$

Proof. The proof is a straightforward computation of the derivatives. \square

Lemma A.5 (Hessian of the loss at small m and r). *Consider $m \in \mathbb{R}^{H \times F}$ in the space orthogonal to $\mathbb{E}\theta$ i.e. $m_h^\top \mathbb{E}\theta = 0$ for all h . Take $r \in \mathcal{S}_+^H$. Assume that b is not specialized, i.e. $b_h = \tilde{b}$ for all h . For the softmax-1 assume that b and v reached the fixed-point described by Lemma A.4 i.e. $Lv = L + e^{\tilde{b}}$. The loss around $m \approx 0$, $r \approx 0$, b and v can be expanded as*

$$\begin{aligned} \tilde{\mathcal{E}}_\sigma(m, r, b + \tilde{b}, v) &= \tilde{\mathcal{E}}_\sigma(0, 0, b, v) + c_1^{(2)} \sum_{h, h'}^H (r^2)_{hh'} + c_5^{(2)} (\tilde{b}^\top \mathbf{1}_H)^2 \\ &+ \left(\mathbf{1}_H \mathbf{1}_H^\top \otimes (c_1^{(2)} I_F + (c_2^{(2)} + c_4^{(2)}) \text{Cov} \theta) - (c_3^{(2)} + c_4^{(2)}) I_H \otimes \text{Cov} \theta \right) \cdot (m, m) + \mathcal{O}((\|r\|_F^2 + \|b\|_2^2 + \|m\|_F^2)^2) \end{aligned} \quad (\text{A20})$$

with \otimes the tensorial product between the spaces \mathbb{R}^H and \mathbb{R}^F , and $c_1^{(2)}, c_2^{(2)}, c_3^{(2)} \in \mathbb{R}$ strictly positive and $c_4^{(2)} \in \mathbb{R}, c_5^{(2)} \in \mathbb{R}$ positive for all $L \geq 3$.

Proof. $\nabla_{r, m}^2 \tilde{\mathcal{E}}_\sigma(0, 0, b, v) = 0$ because the gradient w.r.t. r brings a ξ while the gradient w.r.t. m brings a χ^* . ξ is centered and independent of χ^* thus the expectation is null. The same reasoning holds for $\nabla_{r, b}^2 \tilde{\mathcal{E}}_\sigma(0, 0, b, v) = 0$. We also have $\nabla_{m, b}^2 \tilde{\mathcal{E}}_\sigma(0, 0, b, v) \cdot (m, b) = 0$ because we consider $m \mathbb{E}\theta = 0$.

For the Hessian w.r.t. r we expand the loss around $\chi = r\xi \approx 0$:

$$\tilde{\mathcal{E}}_\sigma(0, r, b, v) = \mathbb{E}_{\epsilon, \xi} \left[\sum_{\ell}^L \left(\delta_{\ell, \epsilon} - \frac{1}{H} \sum_h^H \sigma(r\xi, b, v; h)_\ell \right)^2 \right] \quad (\text{A21})$$

$$= \mathbb{E}_{\epsilon, \xi} \left[\sum_{\ell}^L \left(\delta_{\ell, \epsilon} - \frac{1}{H} \sum_h^H \left(\sigma(0, b, v; h)_\ell + \sum_{h', \ell'} \partial_{h' \ell'} \sigma(0, b, v; h) \ell r_{h'}^\top \xi_{\ell'} + \frac{1}{2} \sum_{h', \ell', h'', \ell''} \partial_{h' \ell' h'' \ell''}^2 \sigma(0, b, v; h) \ell r_{h'}^\top \xi_{\ell'} r_{h''}^\top \xi_{\ell''} \right) \right)^2 \right] \quad (\text{A22})$$

$$= \mathbb{E}_{\epsilon, \xi} \left[\sum_{\ell}^L \left(\delta_{\ell, \epsilon} - H^{-1} \sum_h \sigma(0, b, v; h)_\ell \right)^2 - \sum_{\ell}^L \frac{1}{H} \left(\delta_{\ell, \epsilon} - H^{-1} \sum_h \sigma(0, b, v; h)_\ell \right) \right]$$

$$\times \sum_{h,h',\ell',h'',\ell''} \partial_{h'\ell',h''\ell''}^2 \sigma(0, b, v; h) \ell r_{h'}^\top \xi_{:\ell'} r_{h''}^\top \xi_{:\ell''} + \sum_{\ell} \frac{1}{H^2} \left(\sum_{h,h',\ell'} \partial_{h'\ell'} \sigma(0, b, v; h) \ell r_{h'}^\top \xi_{:\ell'} \right)^2 \Big] \quad (\text{A23})$$

$$= \tilde{\mathcal{E}}_{\sigma}(0, 0, b, v) + \sum_{\ell} \frac{1}{H} \left(H^{-1} \sum_h \sigma(0, b, v; h)_{\ell} - \delta_{\ell,1} \right) \sum_{h,h',h'',\ell'} \partial_{h'\ell',h''\ell''}^2 \sigma(0, b, v; h) \ell r_{h'}^\top r_{h''} \\ + \sum_{\ell} \frac{1}{H^2} \sum_{h_1,h'_1,h_2,h'_2,\ell'} \partial_{h'_1\ell'} \sigma(0, b, v; h_1)_{\ell} \partial_{h'_2\ell'} \sigma(0, b, v; h_2) \ell r_{h'_1}^\top r_{h'_2} \quad (\text{A24})$$

$$= \tilde{\mathcal{E}}_{\sigma}(0, 0, b, v) + \frac{1}{H^2} \sum_{h',h''} \sum_{\ell,\ell'} \left(\sum_h \partial_{h'\ell'} \sigma(0, b, v; h)_{\ell} \right) \left(\sum_h \partial_{h''\ell'} \sigma(0, b, v; h)_{\ell} \right) r_{h'}^\top r_{h''} \quad (\text{A25})$$

where we took the expectation over $\xi_{\ell} \sim \mathcal{N}(0, I_H)$ and discarded the term of order one in r with null expectation. We simplified $\sum_{\ell} (H^{-1} \sum_h \sigma(0, b, v; h)_{\ell} - \delta_{\ell,1}) \times (\text{function independent of } \ell) = 0$, using that b is not specialized and using the fixed-point condition for b and v for the softmax-1. Consequently,

$$\tilde{\mathcal{E}}_{\sigma}(0, r, b, v) = \tilde{\mathcal{E}}_{\sigma}(0, 0, b, v) + c_1^{(2)} \sum_{h',h''} (r^2)_{h'h''} \quad (\text{A26})$$

with the constant

$$c_1^{(2)} = \frac{1}{H^2} \sum_{\ell,\ell'} \left(\sum_h \partial_{1\ell'} \sigma(0, b, v; h)_{\ell} \right)^2 > 0. \quad (\text{A27})$$

We chose the particular index 1 for the derivative because of the permutation invariance with respect to the heads.

For the Hessian w.r.t. m we perform a similar derivation, expanding the loss around $\chi = m\chi^* \approx 0$. We take in account the fact that $\chi_{f\ell}^* \sim \mathcal{N}(\delta_{\ell,\epsilon} \theta_f, 1)$.

$$\tilde{\mathcal{E}}_{\sigma}(m, 0, b, v) = \mathbb{E}_{\epsilon,\theta,\chi^*} \left[\sum_{\ell} \left(\delta_{\ell,\epsilon} - \frac{1}{H} \sum_h \sigma(m\chi^*, b, v; h)_{\ell} \right)^2 \right] \quad (\text{A28})$$

$$= \mathbb{E}_{\epsilon,\theta,\chi^*} \left[\sum_{\ell} \left(\delta_{\ell,\epsilon} - \frac{1}{H} \sum_h \left(\sigma(0, b, v; h)_{\ell} + \sum_{h',\ell'} \partial_{h'\ell'} \sigma(0, b, v; h)_{\ell} m_{h'}^\top \chi_{:\ell'}^* + 1/2 \sum_{h',\ell',h'',\ell''} \partial_{h'\ell',h''\ell''}^2 \sigma(0, b, v; h)_{\ell} m_{h'}^\top \chi_{:\ell'}^* m_{h''}^\top \chi_{:\ell''}^* \right) \right)^2 \right] \quad (\text{A29})$$

$$= \mathbb{E}_{\epsilon,\theta,\chi^*} \left[\sum_{\ell} \left(\delta_{\ell,\epsilon} - H^{-1} \sum_h \sigma(0, b, v; h)_{\ell} \right)^2 - 2 \sum_{\ell} \frac{1}{H} \left(\delta_{\ell,\epsilon} - H^{-1} \sum_h \sigma(0, b, v; h)_{\ell} \right) \sum_{h,h',\ell'} \partial_{h'\ell'} \sigma(0, b, v; h)_{\ell} m_{h'}^\top \chi_{:\ell'}^* \right. \\ \left. - \sum_{\ell} \frac{1}{H} \left(\delta_{\ell,\epsilon} - H^{-1} \sum_h \sigma(0, b, v; h)_{\ell} \right) \sum_{h,h',\ell',h'',\ell''} \partial_{h'\ell',h''\ell''}^2 \sigma(0, b, v; h)_{\ell} m_{h'}^\top \chi_{:\ell'}^* m_{h''}^\top \chi_{:\ell''}^* \right. \\ \left. + \sum_{\ell} \frac{1}{H^2} \left(\sum_{h,h',\ell'} \partial_{h'\ell'} \sigma(0, b, v; h)_{\ell} m_{h'}^\top \chi_{:\ell'}^* \right)^2 \right] \quad (\text{A30})$$

$$= \tilde{\mathcal{E}}_{\sigma}(0, 0, b, v) + 2 \sum_{\ell} \frac{1}{H} \left(H^{-1} \sum_h \sigma(0, b, v; h)_{\ell} - \delta_{\ell,1} \right) \sum_{h,h'} \partial_{h'1} \sigma(0, b, v; h)_{\ell} m_{h'}^\top \mathbb{E} \theta \\ + \sum_{\ell} \frac{1}{H} \left(H^{-1} \sum_h \sigma(0, b, v; h)_{\ell} - \delta_{\ell,1} \right) \sum_{h,h',\ell',h''} \partial_{h'\ell',h''\ell''}^2 \sigma(0, b, v; h)_{\ell} \sum_{f,f'} m_{h'f} m_{h''f'} (\delta_{f,f'} + \delta_{\ell',1} \mathbb{E} \theta_f \theta_{f'}) \\ + \sum_{\ell} \frac{1}{H^2} \sum_{h_1,h'_1,h_2,h'_2,\ell'} \partial_{h'_1\ell'} \sigma(0, b, v; h_1)_{\ell} \partial_{h'_2\ell'} \sigma(0, b, v; h_2)_{\ell} \sum_{f,f'} m_{h'_1f} m_{h'_2f'} (\delta_{f,f'} + \delta_{\ell',1} \mathbb{E} \theta_f \theta_{f'}) \quad (\text{A31})$$

$$\begin{aligned}
&= \tilde{\mathcal{E}}_\sigma(0, 0, b, v) + \sum_\ell \frac{1}{H} \left(H^{-1} \sum_h \sigma(0, b, v; h)_\ell - \delta_{\ell,1} \right) \sum_{h,h',h''} \partial_{h',h''}^2 \sigma(0, b, v; h)_\ell \sum_{f,f'}^F m_{h'f} m_{h''f'} \mathbb{E} \theta_f \theta_{f'} \\
&+ \frac{1}{H^2} \sum_{h,h'} \sum_{\ell,\ell'} \left(\sum_h \partial_{h'\ell'} \sigma(0, b, v; h)_\ell \right) \left(\sum_h \partial_{h''\ell'} \sigma(0, b, v; h)_\ell \right) \sum_{f,f'}^F m_{h'f} m_{h''f'} (\delta_{f,f'} + \delta_{\ell',1} \mathbb{E} \theta_f \theta_{f'})
\end{aligned} \tag{A32}$$

We consider the space orthogonal to $\mathbb{E}\theta$, i.e. $m_{h'}^\top \mathbb{E}\theta = 0$ for all h . We simplified $\sum_\ell^L (H^{-1} \sum_h \sigma(0, b, v; h)_\ell - \delta_{\ell,1}) \times$ (function independent of ℓ) = 0. We introduce the covariance of θ . Consequently,

$$\tilde{\mathcal{E}}_\sigma(m, 0, b, v) = \tilde{\mathcal{E}}_\sigma(0, 0, b, v) + c_1^{(2)} \sum_{h',h''} m_{h'}^\top m_{h''} + (c_2^{(2)} + c_4^{(2)}) \sum_{h',h''} m_{h'}^\top \text{Cov}(\theta) m_{h''} - (c_3^{(2)} + c_4^{(2)}) \sum_{h'} m_{h'}^\top \text{Cov}(\theta) m_{h'} \tag{A33}$$

$$c_1^{(2)} = \frac{1}{H^2} \sum_{\ell,\ell'} \left(\sum_h \partial_{1\ell'} \sigma(0, b, v; h)_\ell \right)^2 > 0 \tag{A34}$$

$$c_2^{(2)} = \frac{1}{H^2} \sum_{\ell,\ell'} \left(\sum_h \partial_{11} \sigma(0, b, v; h)_\ell \right)^2 > 0 \tag{A35}$$

$$c_3^{(2)} = -\frac{1}{H} \sum_\ell^L \left(H^{-1} \sum_h \sigma(0, b, v; h)_\ell - \delta_{\ell,1} \right) \sum_h \partial_{11,11}^2 \sigma(0, b, v; h)_\ell \tag{A36}$$

$$c_4^{(2)} = \frac{1}{H} \sum_\ell^L \left(H^{-1} \sum_h \sigma(0, b, v; h)_\ell - \delta_{\ell,1} \right) \sum_h \partial_{11,21}^2 \sigma(0, b, v; h)_\ell \tag{A37}$$

so the loss is

$$\tilde{\mathcal{E}}_\sigma(m, 0, b, v) = \tilde{\mathcal{E}}_\sigma(0, 0, b, v) + \left(\mathbf{1}_H \mathbf{1}_H^\top \otimes (c_1^{(2)} I_F + (c_2^{(2)} + c_4^{(2)}) \text{Cov} \theta) - (c_3^{(2)} + c_4^{(2)}) I_H \otimes \text{Cov} \theta \right) \cdot (m, m). \tag{A38}$$

Between $c_3^{(2)}$ and $c_4^{(2)}$ we distinguished the cases $h' = h''$ and $h' \neq h''$. We compute these two constants for the different activation functions. We have

σ	$c_3^{(2)}$	$c_4^{(2)}$
softmax	$H^{-1}(L-1)L^{-2}(1-2L^{-1})$	0
softmax-1	$vH^{-1}(L-1)L^{-1}(L+e^{\tilde{b}})^{-1}(1-2(L+e^{\tilde{b}})^{-1})$	0
B-softmax	$H^{-1}(L-1)L^{-2}(1-2(HL)^{-1})$	$(L-1)L^{-1}2(HL)^{-2}$

Consequently for all $L \geq 3$ one has $c_3^{(2)} > 0$ and $c_4^{(2)} \geq 0$.

For the Hessian w.r.t. b we compute that for the softmax-1

$$\partial_{b_h, b_h'}^2 \tilde{\mathcal{E}}_\sigma(0, 0, b, v) = 2 \frac{v^2 L}{H^2} \frac{e^{2\tilde{b}}}{(L+e^{\tilde{b}})^4} \tag{A39}$$

and for the B-softmax

$$\partial_{b_h, b_h'}^2 \tilde{\mathcal{E}}_\sigma(0, 0, b, v) = 0. \tag{A40}$$

□

Lemma A.6 (Hessian of the loss at small but finite m). *We take σ softmax. We assume that $\mathbb{E}\theta = 0$ and that the θ_f are independent. Let n be an integer, $\bar{f}_1, \dots, \bar{f}_n \in [F]^n$ all different, $\bar{m} \in \mathbb{R}^{H \times F}$ and assume that $\bar{m}_{\cdot f} = 0$ for all $f \notin \{\bar{f}_1, \dots, \bar{f}_n\}$. Pick $f \notin \{\bar{f}_1, \dots, \bar{f}_n\}$; then the Hessian of the loss is*

$$\nabla_{m_{\cdot f}, m_{\cdot f}}^2 \tilde{\mathcal{E}}_\sigma(\bar{m}, 0, 0, 0) = \nabla_{m_{\cdot f}, m_{\cdot f}}^2 \tilde{\mathcal{E}}_\sigma(0, 0, 0, 0) + \sum_i^n c_{1,i}^{(4)} \|\bar{m}_{\cdot \bar{f}_i}\|_2^2 I_H \tag{A41}$$

$$+ \sum_i^n c_{2,i}^{(4)} \text{Diag}(\bar{m}_{:\bar{f}_i}^{\odot 2}) + \sum_i^n c_{3,i}^{(4)} \bar{m}_{:\bar{f}_i} \bar{m}_{:\bar{f}_i}^\top + M + \mathcal{O}(\|\bar{m}\|_F^4)$$

where M is a quadratic form that cancels when $m_{:\bar{f}}^\top \mathbf{1}_H = 0$ and $\bar{m}^\top \mathbf{1}_H = 0$, and where $c_{1,i}^{(4)} > 0, c_{2,i}^{(4)} \in \mathbb{R}, c_{3,i}^{(4)} > 0$ for all $L \geq 3$ does not depend on \bar{m} .

Proof. The proof is a Taylor expansion of the loss to the 2nd order in m_f around \bar{m} and to the 2nd order in \bar{m} around 0. We take $m \in \mathbb{R}^{H \times F}$ with $m_{\bar{f}_i} = 0$ for all \bar{f}_i ; it encompasses the case of a matrix where only the f -th column is not null equal to m_f . Since we consider σ softmax, to lighten the notation we write $\sigma(\chi_h)$ for $\sigma(\chi, b, v; h)$.

$$\tilde{\mathcal{E}}_\sigma(m + \bar{m}, 0, 0, 0) = \mathbb{E}_{\epsilon, \theta, \chi^*} \left[\sum_\ell^L \left(\delta_{\ell, \epsilon} - \frac{1}{H} \sum_h^H \sigma(m_h^\top \chi^*)_\ell \right)^2 \right] \quad (\text{A42})$$

$$= \mathbb{E}_{\epsilon, \theta, \chi^*} \left[\sum_\ell^L \left(\delta_{\ell, \epsilon} - \frac{1}{H} \sum_h^H \left(\sigma(\bar{m}_h^\top \chi^*)_\ell + \sum_{\ell'} \partial_{\ell'} \sigma(\bar{m}_h^\top \chi^*)_\ell m_h^\top \chi_{:\ell'}^* + \frac{1}{2} \sum_{\ell', \ell''} \partial_{\ell' \ell''}^2 \sigma(\bar{m}_h^\top \chi^*)_\ell m_h^\top \chi_{:\ell'}^* m_h^\top \chi_{:\ell''}^* \right) \right)^2 \right] \quad (\text{A43})$$

$$= \mathbb{E}_{\epsilon, \theta, \chi^*} \left[\sum_\ell^L \left(\delta_{\ell, \epsilon} - \frac{1}{H} \sum_h^H \sigma(\bar{m}_h^\top \chi^*)_\ell \right)^2 - 2 \sum_\ell^L \left(\delta_{\ell, \epsilon} - \frac{1}{H} \sum_h^H \sigma(\bar{m}_h^\top \chi^*)_\ell \right) \frac{1}{H} \sum_{h, \ell'} \partial_{\ell'} \sigma(\bar{m}_h^\top \chi^*)_\ell m_h^\top \chi_{:\ell'}^* \right] \quad (\text{A44})$$

$$- \sum_\ell^L \left(\delta_{\ell, \epsilon} - \frac{1}{H} \sum_h^H \sigma(\bar{m}_h^\top \chi^*)_\ell \right) \frac{1}{H} \sum_{h, \ell', \ell''} \partial_{\ell' \ell''}^2 \sigma(\bar{m}_h^\top \chi^*)_\ell m_h^\top \chi_{:\ell'}^* m_h^\top \chi_{:\ell''}^* + \sum_\ell^L \frac{1}{H^2} \left(\sum_{h, \ell'} \partial_{\ell'} \sigma(\bar{m}_h^\top \chi^*)_\ell m_h^\top \chi_{:\ell'}^* \right)^2 \right]$$

$$= \tilde{\mathcal{E}}_\sigma(\bar{m}, 0, 0, 0) + \underbrace{-2 \mathbb{E}_{\epsilon, \theta, \chi^*} \sum_\ell^L \left(\delta_{\ell, \epsilon} - \frac{1}{H} \sum_h^H \sigma(\bar{m}_h^\top \chi^*)_\ell \right) \frac{1}{H} \sum_h \partial_1 \sigma(\bar{m}_h^\top \chi^*)_\ell m_h^\top \mathbb{E} \theta}_{=0} \quad (\text{A45})$$

$$- \underbrace{\mathbb{E}_{\epsilon, \theta, \chi^*} \sum_\ell^L \left(\delta_{\ell, \epsilon} - \frac{1}{H} \sum_h^H \sigma(\bar{m}_h^\top \chi^*)_\ell \right) \frac{1}{H} \sum_{h, \ell'} \partial_{\ell' \ell''}^2 \sigma(\bar{m}_h^\top \chi^*)_\ell \sum_{f, f'}^F m_{hf} m_{hf'} (\delta_{f, f'} + \delta_{\ell', 1} \mathbb{E} \theta_f \theta_{f'})}_{(1)}$$

$$+ \underbrace{\mathbb{E}_{\epsilon, \theta, \chi^*} \sum_\ell^L \frac{1}{H^2} \sum_{h, h', \ell'} \partial_{\ell'} \sigma(\bar{m}_h^\top \chi^*)_\ell \partial_{\ell'} \sigma(\bar{m}_{h'}^\top \chi^*)_{\ell'} \sum_{f, f'}^F m_{hf} m_{h'f'} (\delta_{f, f'} + \delta_{\ell', 1} \mathbb{E} \theta_f \theta_{f'})}_{(2)}$$

where we used the independence of the θ_f to factorize the expectation. We expand with respect to \bar{m} , discarding the 1st order terms because $\mathbb{E} \theta = 0$.

$$(1) = c_2^{(2)} \sum_h m_h^\top \text{Cov}(\theta) m_h + \mathbb{E}_{\epsilon, \theta, \chi^*} \sum_\ell^L \frac{1}{2H} \sum_{h', \ell'', \ell'''} \partial_{\ell' \ell'' \ell'''}^2 \sigma(0)_\ell \bar{m}_{h'}^\top \chi_{:\ell'}^* \bar{m}_{h'}^\top \chi_{:\ell''}^* \frac{1}{H} \sum_{h, \ell'} \partial_{\ell' \ell''}^2 \sigma(0)_\ell m_h^\top (I_F + \delta_{\ell', 1} \text{Cov}(\theta)) m_h$$

$$+ \underbrace{\mathbb{E}_{\epsilon, \theta, \chi^*} \sum_\ell^L \frac{1}{H} \sum_{h', \ell'''} \partial_{\ell'''} \sigma(0)_\ell \bar{m}_{h'}^\top \chi_{:\ell'''}^* \frac{1}{H} \sum_{h, \ell', \ell''} \partial_{\ell' \ell'' \ell'''}^3 \sigma(0)_\ell \bar{m}_h^\top \chi_{:\ell'}^* m_h^\top (I_F + \delta_{\ell', 1} \text{Cov}(\theta)) m_h}_{=0}$$

$$+ \mathbb{E}_{\epsilon, \theta, \chi^*} \sum_\ell^L (\sigma(0)_\ell - \delta_{\ell, 1}) \frac{1}{2H} \sum_{h, \ell', \ell'', \ell'''} \partial_{\ell' \ell'' \ell'''}^4 \sigma(0)_\ell \bar{m}_h^\top \chi_{:\ell'}^* \bar{m}_h^\top \chi_{:\ell''}^* m_h^\top (I_F + \delta_{\ell', 1} \text{Cov}(\theta)) m_h \quad (\text{A46})$$

$$= c_2^{(2)} \sum_h m_h^\top \text{Cov}(\theta) m_h + \sum_\ell^L \frac{1}{2H^2} \sum_{h', \ell''} \partial_{\ell' \ell''}^2 \sigma(0)_\ell \bar{m}_h^\top (I_F + \delta_{\ell', 1} \text{Cov}(\theta)) \bar{m}_{h'} \sum_{h, \ell'} \partial_{\ell' \ell''}^2 \sigma(0)_\ell m_h^\top (I_F + \delta_{\ell', 1} \text{Cov}(\theta)) m_h$$

$$+ \sum_\ell^L (\sigma(0)_\ell - \delta_{\ell, 1}) \sum_{\ell', \ell''} \frac{1}{2H} \sum_h \partial_{\ell' \ell''}^4 \sigma(0)_\ell \bar{m}_h^\top (I_F + \delta_{\ell', 1} \text{Cov}(\theta)) \bar{m}_h m_h^\top (I_F + \delta_{\ell', 1} \text{Cov}(\theta)) m_h \quad (\text{A47})$$

$$\begin{aligned}
&= c_2^{(2)} \sum_h m_h^\top \text{Cov}(\theta) m_h + \sum_\ell \frac{1}{2H^2} \sum_{h'} \partial_{1,1}^2 \sigma(0)_\ell \bar{m}_{h'}^\top \text{Cov}(\theta) \bar{m}_{h'} \sum_h \partial_{1,1}^2 \sigma(0)_\ell m_h^\top \text{Cov}(\theta) m_h \\
&\quad + \sum_\ell (\sigma(0)_\ell - \delta_{\ell,1}) \sum_{\ell', \ell''} \frac{1}{2H} \sum_h \partial_{\ell', \ell''}^4 \sigma(0)_\ell \bar{m}_h^\top (I_F + \delta_{\ell',1} \text{Cov} \theta) \bar{m}_h m_h^\top (I_F + \delta_{\ell',1} \text{Cov} \theta) m_h
\end{aligned} \tag{A48}$$

where we discarded a term because of $\bar{m}_{:f}^\top \mathbf{1}_H = 0$ and used that $\sum_{\ell'} \partial_{\ell', \ell'}^2 \sigma(0)_\ell = 0$ for all ℓ . Consequently there are constants $\tilde{c}_{1,i}^{(4)} > 0, \tilde{c}_{2,i}^{(4)}, \tilde{c}_{3,i}^{(4)} \in \mathbb{R}$ for all $L \geq 3$ independent of \bar{m} such that

$$\begin{aligned}
(1) &= c_2^{(2)} (I_H \otimes \text{Cov} \theta) \cdot (m, m) + \sum_i^n \tilde{c}_{1,i}^{(4)} \|\bar{m}_{:\bar{f}_i}\|_2^2 (I_H \otimes \text{Cov} \theta) \cdot (m, m) \\
&\quad + \sum_i^n \text{Diag}(\bar{m}_{:\bar{f}_i}^{\otimes 2}) \otimes (\tilde{c}_{2,i}^{(4)} I_F + \tilde{c}_{3,i}^{(4)} \text{Cov} \theta) \cdot (m, m).
\end{aligned} \tag{A49}$$

Turning to the second term,

$$\begin{aligned}
(2) &= c_1^{(2)} \sum_{h, h'} m_h^\top m_{h'} + c_3^{(2)} \sum_{h, h'} m_h^\top \text{Cov}(\theta) m_{h'} \\
&\quad + \sum_\ell \frac{1}{H^2} \sum_{h, h', \ell', \ell''} \partial_{\ell', \ell''}^2 \sigma(0)_\ell \partial_{\ell', \ell''}^2 \sigma(0)_\ell \bar{m}_h^\top (I_F + \delta_{\ell',1} \text{Cov}(\theta)) \bar{m}_{h'} m_h^\top (I_F + \delta_{\ell',1} \text{Cov}(\theta)) m_{h'}
\end{aligned} \tag{A50}$$

where we kept only terms with even number of h and h' because of $m_{:f}^\top \mathbf{1}_H = 0$ and took the expectation. Consequently there are constants $\tilde{c}_{4,i}^{(4)} > 0, \tilde{c}_{5,i}^{(4)} > 0$ for all $L \geq 2$ independent of \bar{m} such that

$$(2) = \mathbf{1}_H \mathbf{1}_H^\top \otimes (c_1^{(2)} I_F + c_3^{(2)} \text{Cov} \theta) \cdot (m, m) + \sum_i^n \bar{m}_{:\bar{f}_i} \bar{m}_{:\bar{f}_i}^\top \otimes (\tilde{c}_{4,i}^{(4)} I_F + \tilde{c}_{5,i}^{(4)} \text{Cov} \theta) \cdot (m, m). \tag{A51}$$

Assembling the two parts together we obtain

$$\begin{aligned}
\tilde{\mathcal{E}}_\sigma(m + \bar{m}, 0, 0, 0) &= \tilde{\mathcal{E}}_\sigma(\bar{m}, 0, 0, 0) + \tilde{\mathcal{E}}_\sigma(m, 0, 0, 0) - \tilde{\mathcal{E}}_\sigma(0, 0, 0, 0) + \sum_i^n \tilde{c}_{1,i}^{(4)} \|\bar{m}_{:\bar{f}_i}\|_2^2 (I_H \otimes \text{Cov} \theta) \cdot (m, m) \\
&\quad + \sum_i^n \text{Diag}(\bar{m}_{:\bar{f}_i}^{\otimes 2}) \otimes (\tilde{c}_{2,i}^{(4)} I_F + \tilde{c}_{3,i}^{(4)} \text{Cov} \theta) \cdot (m, m) + \sum_i^n \bar{m}_{:\bar{f}_i} \bar{m}_{:\bar{f}_i}^\top \otimes (\tilde{c}_{4,i}^{(4)} I_F + \tilde{c}_{5,i}^{(4)} \text{Cov} \theta) \cdot (m, m) + \mathcal{O}(\|\bar{m}\|_F^4, \|m\|_F^4).
\end{aligned} \tag{A52}$$

For a particular feature f and a particular magnetization $m_{:f}$ we extract the corresponding term to obtain

$$\begin{aligned}
\nabla_{m_f, m_f}^2 \tilde{\mathcal{E}}_\sigma(\bar{m}, 0, 0, 0) &= \nabla_{m_f, m_f}^2 \tilde{\mathcal{E}}_\sigma(0, 0, 0, 0) + \sum_i^n c_{1,i}^{(4)} \|\bar{m}_{:\bar{f}_i}\|_2^2 I_H \\
&\quad + \sum_i^n c_{2,i}^{(4)} \text{Diag}(\bar{m}_{:\bar{f}_i}^{\otimes 2}) + \sum_i^n c_{3,i}^{(4)} \bar{m}_{:\bar{f}_i} \bar{m}_{:\bar{f}_i}^\top + M + \mathcal{O}(\|\bar{m}\|_F^4)
\end{aligned} \tag{A53}$$

with $c_{1,i}^{(4)} = \text{Var}(\theta_f) \tilde{c}_{1,i}^{(4)}$, $c_{2,i}^{(4)} = \tilde{c}_{2,i}^{(4)} + \tilde{c}_{3,i}^{(4)} \text{Var}(\theta_f)$ and $c_{3,i}^{(4)} = \tilde{c}_{4,i}^{(4)} + \tilde{c}_{5,i}^{(4)} \text{Var}(\theta_f)$. \square

3. Expressiveness and performances of different activation functions

In this part we derive the results about the Bayes risk and the expressivity of the softmax and softmax-1 activation functions.

Proof of Proposition IV.1. The Bayes-optimal estimator is the posterior mean under our probabilistic model. It is given by the conditional probability $P(\epsilon = \ell | X, \{k_f^*\}_{f \in [F]})$, which we can compute using the Bayes formula:

$$P(\epsilon = \ell | X, \{k_f^*\}_{f \in [F]}) = \frac{P(\epsilon = \ell, X | \{k_f^*\}_{f \in [F]})}{P(X | \{k_f^*\}_{f \in [F]})}.$$

The numerator is computed as

$$\begin{aligned} P(\epsilon = \ell, X | \{k_f^*\}_{f \in [F]}) &= \int_{\theta} P(\epsilon = \ell, \theta, X | \{k_f^*\}_{f \in [F]}) d\theta \\ &= \int_{\theta} P(X | \epsilon = \ell, \theta, \{k_f^*\}_{f \in [F]}) P(\epsilon = \ell) P(\theta) d\theta, \end{aligned}$$

where

$$\begin{aligned} P(X | \epsilon = \ell, \theta, \{k_f^*\}_{f \in [F]}) &= \frac{1}{Z} e^{-\frac{\|x_{\ell} - \sum_f \theta_f k_f^*\|_2^2}{2}} \prod_{\ell' \neq \ell}^L e^{-\frac{\|x_{\ell'}\|_2^2}{2}} \\ &= \exp\left(-\frac{\|\sum_f \theta_f k_f^*\|_2^2 - 2X_{\ell}^T(\sum_f \theta_f k_f^*)}{2}\right) \frac{1}{Z} \prod_{\ell'}^L e^{-\frac{\|x_{\ell'}\|_2^2}{2}} = \exp\left(-\frac{\|\theta\|_2^2}{2}\right) \exp X_{\ell}^T(\hat{k}(\theta)) \cdot \frac{1}{Z} \prod_{\ell'}^L e^{-\frac{\|x_{\ell'}\|_2^2}{2}}. \end{aligned}$$

And denominator is a sum over ℓ' of the conditional $P(\epsilon = \ell, X | \{k_f^*\}_{f \in [F]})$. Combining it all together, we get

$$P(\epsilon = \ell | X, \{k_f^*\}_{f \in [F]}) = \frac{\int_{\theta} \exp\left(-\frac{\|\theta\|_2^2}{2}\right) \exp X_{\ell}^T(\hat{k}(\theta)) P(\theta) d\theta}{\sum_{\ell'}^L \int_{\theta} \exp\left(-\frac{\|\theta\|_2^2}{2}\right) \exp X_{\ell'}^T(\hat{k}(\theta)) P(\theta) d\theta}.$$

□

Proof of Proposition IV.3. We show that the softmax attention is not well specified for our data model, while the softmax-1 is well specified.

The intuition is that for softmax one head cannot be good at the same time on a spike \hat{k} and on the opposite $-\hat{k}$, and has to return noise in some cases. Assume that the softmax attention is well-specified, i.e. the reparameterized loss is $\tilde{\mathcal{E}}_{\sigma}(m, r, 0, 0) \approx 0$. Take disjoint $S \subset \mathbb{R}^F$ and $\bar{S} = \{-\theta, \theta \in S\}$ such that $P_{\theta}(S) > 0$ and $P_{\theta}(\bar{S}) > 0$. Recall that by our characterization

$$\begin{aligned} \tilde{\mathcal{E}}_{\sigma}(m, r, 0, 0) &= \mathbb{E}_{\epsilon, \theta, \chi, \xi} \left[\sum_{\ell}^L \left(\delta_{\ell, \epsilon} - \frac{1}{H} \sum_h^H \sigma(\chi_h)_{\ell} \right)^2 \right] \approx 0 \\ \chi_{h\ell} &= \sum_f^F m_{hf} \chi_{f\ell}^* + \sum_{h'}^H r_{hh'} \xi_{h'} \end{aligned}$$

Then for any head h one must have $\sigma(\chi_h)_{\epsilon} \approx 1$ almost surely, i.e. all the heads completely focus on the relevant token ϵ . Consider a $\theta \in S$. This requires that $\chi_{h\epsilon} \gg 1$ and $\sum_f^F m_{hf} \chi_{f\epsilon}^* \gg 1$ a.s. with respect to the randomness of $\chi_{\epsilon}^* \sim (\theta, I_F)$, and thus $\sum_f^F m_{hf} \theta_f \gg 1$, i.e. all the heads are positively aligned towards θ . Considering the opposite spike $-\theta$, one obtains that $\chi_{h\epsilon} \ll -1$ and $\sigma(\chi_h)_{\epsilon} \approx 1/L$, the head does not focus on the relevant token. One obtains a contradiction, $\tilde{E}(m, r) > 0$ and the softmax is not well specified.

Instead, the softmax-1 is well specified, because it allows a head not to return noise in case it is not well aligned with any token. Consider a large signal $\|\theta\|_2 > B$, $B \rightarrow \infty$, and take $H = 2$ opposite heads $m_1 \in \mathbb{R}^F$ and $m_2 = -m_1$. Assume that m_1 is chosen such that the hyperplane $m_1^{\top} \theta = 0$ has a null probability. Take $b_1 = b_2 = B^{3/2}$ the biases of the softmax-1, $v = H$, and scale m_1 and m_2 as B . By symmetry assume that $m_1^{\top} \theta > 0$. Then one has the scalings

$$\begin{aligned} \chi_{1\epsilon} &= m_1^{\top} \theta + \mathcal{O}(B) = \Theta(B^2) & \chi_{1, \ell \neq \epsilon} &= m_1^{\top} \chi_{\ell}^* + \mathcal{O}(1) = \Theta(B) \\ \chi_{2\epsilon} &= m_2^{\top} \theta + \mathcal{O}(B) \ll -1 & \chi_{2, \ell \neq \epsilon} &= m_2^{\top} \chi_{\ell}^* + \mathcal{O}(1) = \Theta(B) \end{aligned}$$

Consequently the attention scores are

$$\begin{aligned} \sigma(\chi_1)_{\epsilon} &= \frac{e^{\Theta(B^2)}}{e^{\Theta(B^3/2)} + e^{\Theta(B^2)} + e^{\Theta(B)}} \rightarrow 1 & \sigma(\chi_1)_{\ell \neq \epsilon} &= \frac{e^{\Theta(B)}}{e^{\Theta(B^3/2)} + e^{\Theta(B)}} \rightarrow 0 & \sigma(\chi_2)_{\ell} &\rightarrow 0 \quad \ell \in [L] \\ \frac{1}{H} \sum_h^H \sigma(\chi_h)_{\epsilon} &\rightarrow 1 & \frac{1}{H} \sum_h^H \sigma(\chi_h)_{\ell \neq \epsilon} &\rightarrow 0 \end{aligned}$$

and $\tilde{\mathcal{E}}_{\sigma}(m, r, b, v) = 0$.

□

Appendix B: Numerical simulation details

We provide the code to run our predictions in the supplementary material.

For the reparametrized population loss $\tilde{\mathcal{E}}$ estimation we discretize the flow with a step size $\delta = 0.02$. We use Monte Carlo integration with 10^5 samples to compute the expectations. We keep the same samples for each step of the gradient descent, which doesn't affect the behavior of the model as can be seen in Fig. 8.

For the initialization, when not comparing to SGD, we add initial noise $\mathcal{N}(0, 10^{-4})$ to m and r , which allows to break the initial symmetry in the parameters. When comparing to SGD we initialize m and r to their empirical values. For SGD and the loss \mathcal{E} , we take $N_b = D$ and learning rate $\gamma = 0.02$.

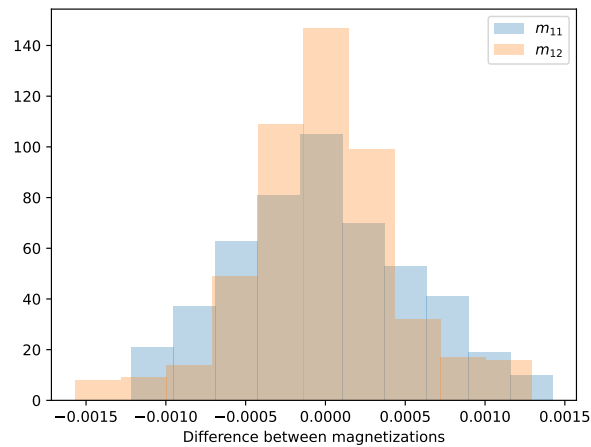


FIG. 8. Histogram of the differences between magnetizations of the first head in the model trained with changed MC samples and the same MC samples at each step of the training. The data are sampled from the flipping spike distribution, $H = 2, F = 2, \nu_1 = \nu_2 = 2, L = 8$.

Appendix C: Supplementary figures

1. Characterization of the training dynamics

We compare our theoretical prediction, Prop. III.2, to the numerical simulation of SGD at finite large D . We consider the different activation functions, on the flipping spike or non-isotropic Gaussian.

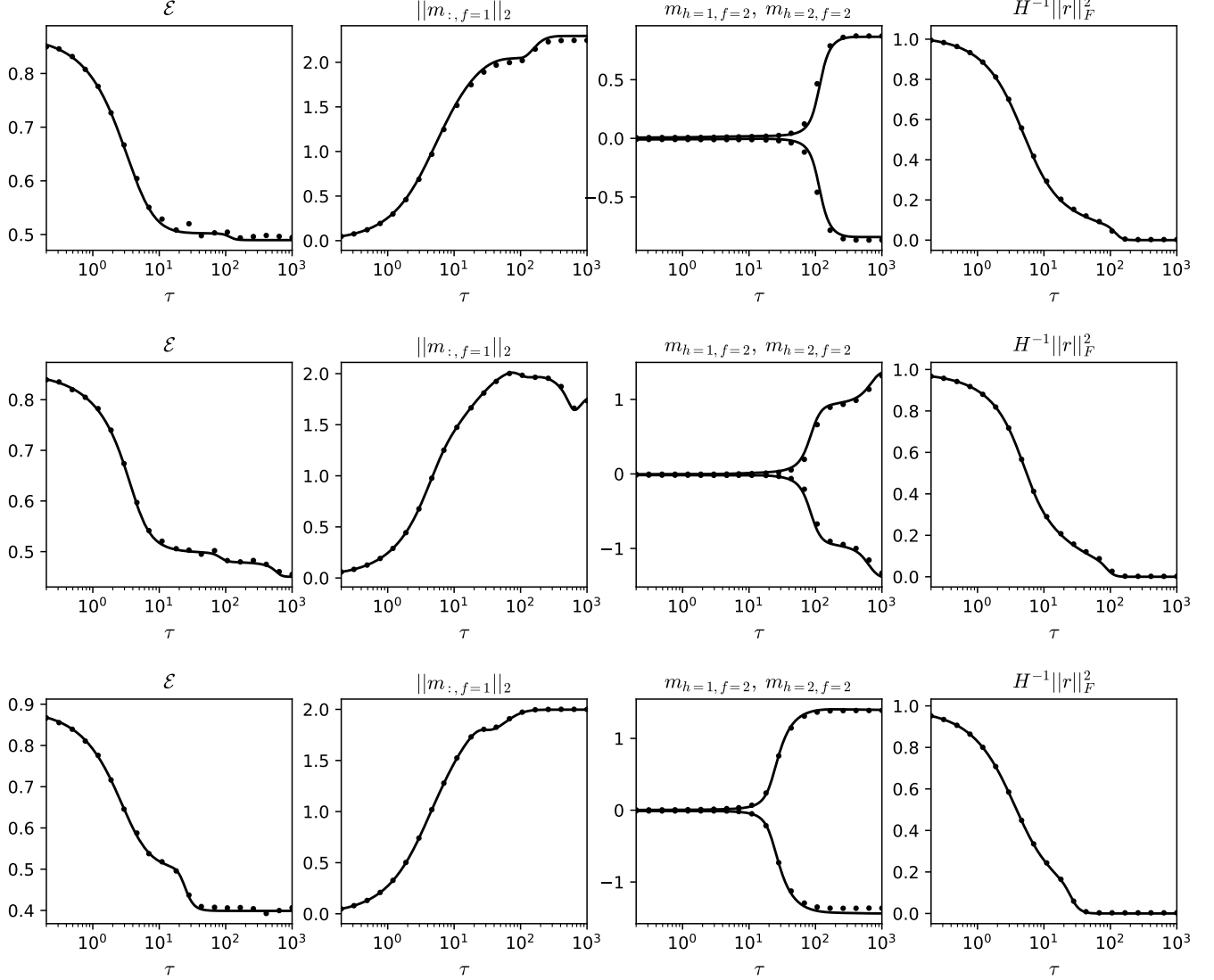


FIG. 9. Asymptotic description of the attention trained by SGD. We compare numerical simulations at finite $D = 10^4$ (dots) and the theoretical description stated in proposition III.2 (continuous lines). We consider sequence length $L = 5$, $H = 2$ heads, $F = 2$ features and θ distributed according to the flipping spike distribution, with signal strengths $\nu_1 = \nu_2 = 2$. Initialization $\eta = 1$. Top: softmax; middle: softmax-1; bottom: B-softmax.

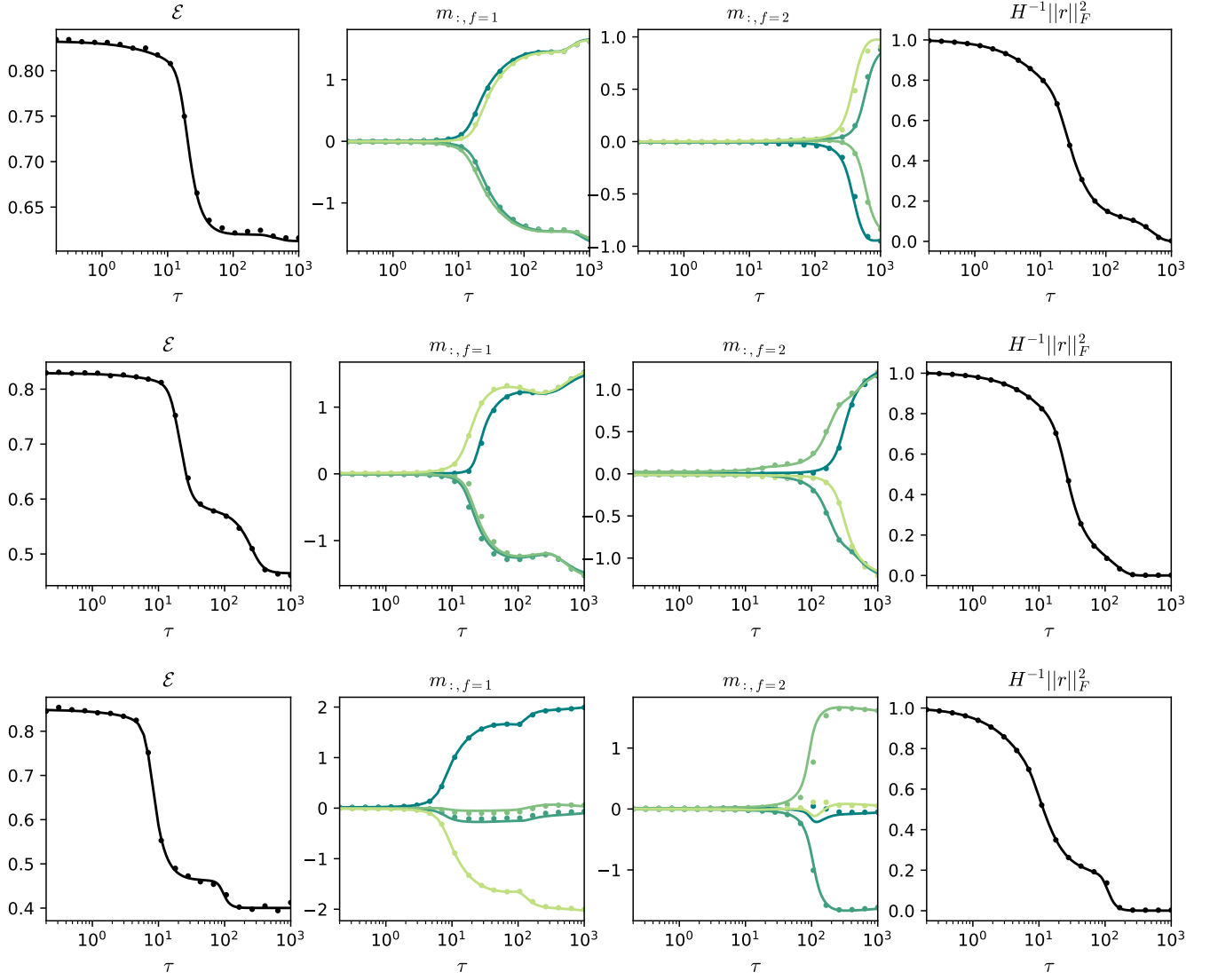


FIG. 10. Asymptotic description of the attention trained by SGD. We compare numerical simulations at finite $D = 10^4$ (dots) and the theoretical description stated in proposition III.2 (continuous lines). We consider sequence length $L = 5$, $H = 4$ heads, $F = 2$ features and θ distributed according to the non-isotropic Gaussian distribution, with signal strengths $\nu_1 = 8, \nu_2 = 2$. Initialization $\eta = 1$. Top: softmax; middle: softmax-1; bottom: B-softmax.

2. Specialization of the heads

We provide additional figures illustrating the specialization of the heads for the flipping spike distribution, depending on the signal strength ν_1 of the average direction and the signal strength ν_2 of the flipping-sign direction.

The specialization of the two heads is measured as their cosine similarity and is reported in Fig. 11 for the softmax. It shows that the specialization grows monotonically with ν_1 and decreases monotonically with ν_2 , as expected.

Notice that when the signal strength in the average and flipping-sign directions are varied, softmax-1 activation exhibits behavior similar to softmax (compare Figs. 12 and 13) with heads being more impacted by the increase of the average direction weights, but the Bayes-softmax reaches the alignment with the hidden spikes even when the signal in the flipping-sign direction is significantly smaller than in the average direction (Fig. 14).

a. Softmax attention

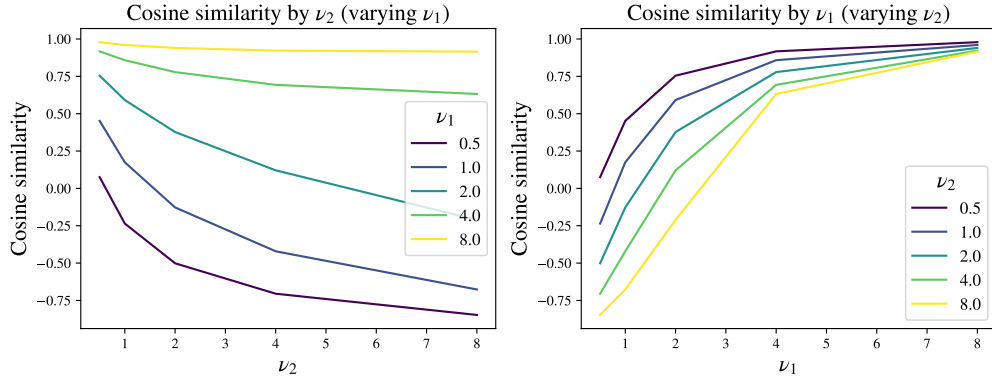


FIG. 11. Cosine similarity between heads for softmax attention with $H = 2$, and flipping spike distribution with $F = 2$, $L = 4$ depending on the signal strengths for the constant and flipping-sign directions.

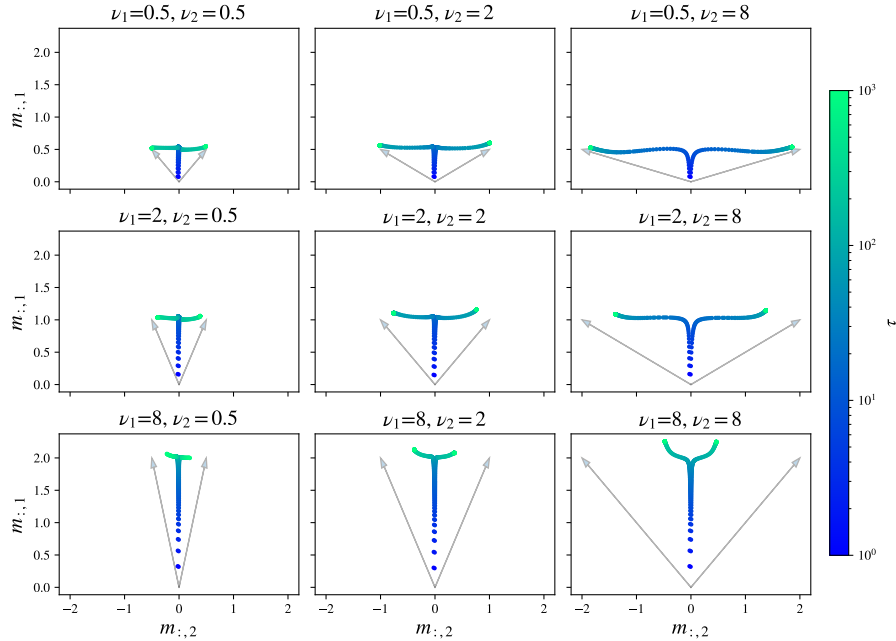


FIG. 12. Evolution of the heads for softmax attention with $H = 2$, and flipping spike distribution with $F = 2$, $L = 4$, with varying values of signal strength for the constant and flipping-sign directions. $\eta = 1$.

b. *Softmax-1 and B-softmax attentions*

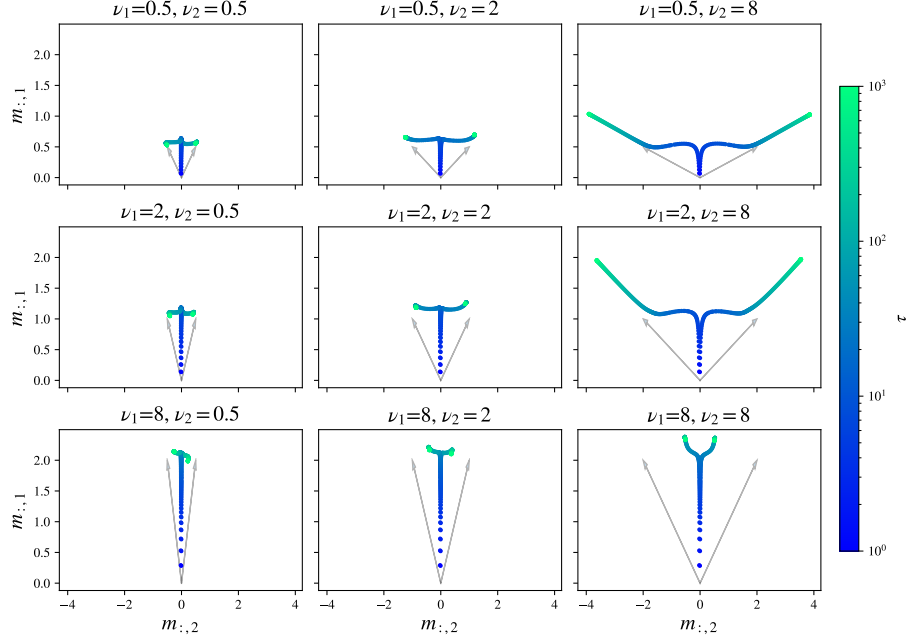


FIG. 13. Evolution of the heads for softmax-1 attention with $H = 2$, and flipping spike distribution with $F = 2$, $L = 4$, with varying values of signal strength for the constant and flipping-sign directions. $\eta = 1$.

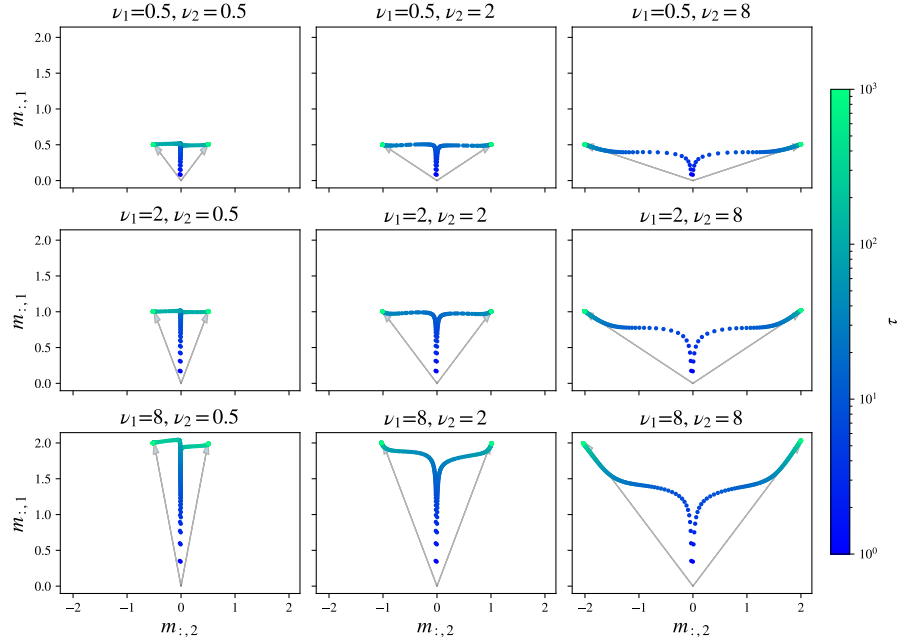


FIG. 14. Evolution of the heads for B-softmax attention with $H = 2$, and flipping spike distribution with $F = 2$, $L = 4$, with varying values of signal strength for the constant and flipping-sign directions. $\eta = 1$.

3. Evolution of the magnetizations of the heads

We provide additional figures illustrating the dynamics of the heads, for various H , σ and P_θ .

a. Softmax attention

The figure 15 shows that when increasing the number of heads H , some heads specialize and diverge more from the average direction, more than at lower H .

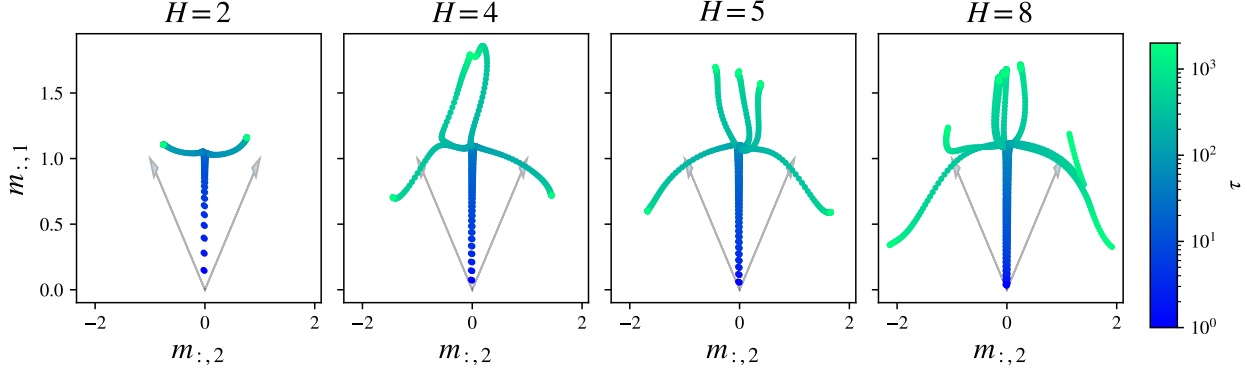


FIG. 15. Evolution of the heads in the model of attention with varying number of heads $H \in \{2, 4, 5, 8\}$, and flipping spike distribution with $F = 2$, $L = 4$, with signal strengths $\nu_1 = \nu_2 = 2$. $\eta = 1$.

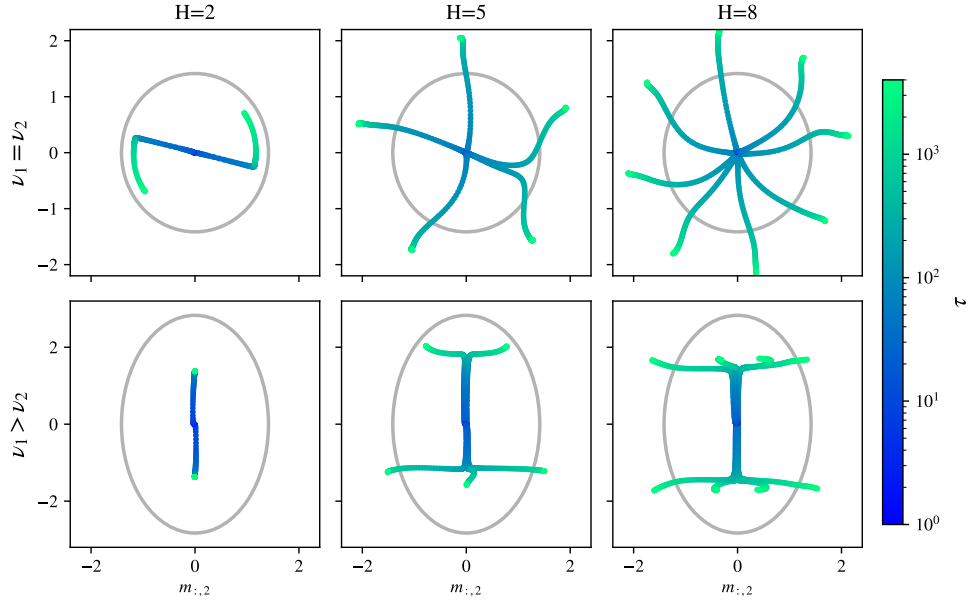


FIG. 16. Evolution of the heads for softmax attention with varying number of heads $H \in \{2, 5, 8\}$, and non-isotropic Gaussian distribution with $F = 2$, $L = 4$, with signal strengths $\nu_1 = \nu_2 = 2$ (top) and $\nu_1 = 8, \nu_2 = 2$ (bottom). $\eta = 1$.

b. *Softmax-1 and B-softmax attentions*

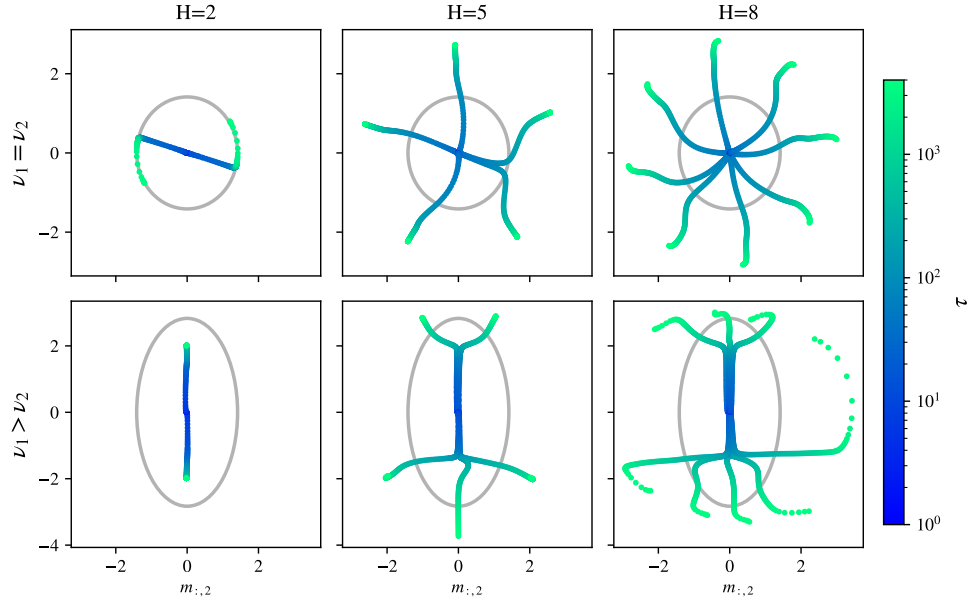


FIG. 17. Evolution of the heads for softmax-1 attention with varying number of heads $H \in \{2, 4, 5, 8\}$, and non-isotropic Gaussian distribution with $F = 2$, $L = 4$, with signal strengths $\nu_1 = \nu_2 = 2$ (top) and $\nu_1 = 8, \nu_2 = 2$ (bottom). $\eta = 1$.

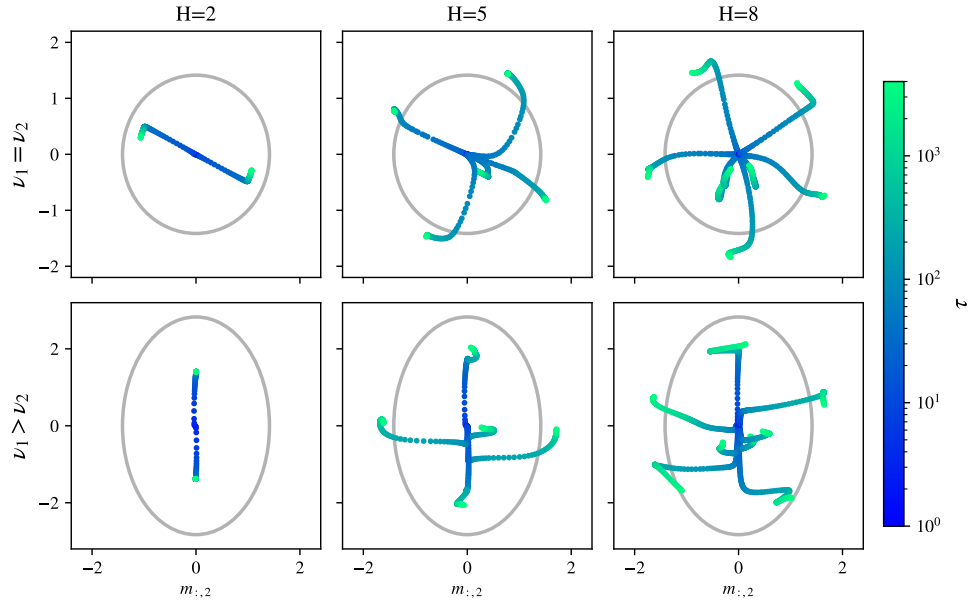


FIG. 18. Evolution of the heads for B-softmax attention with varying number of heads $H \in \{2, 5, 8\}$, and non-isotropic Gaussian distribution with $F = 2$, $L = 4$, with signal strengths $\nu_1 = \nu_2 = 2$ (top) and $\nu_1 = 8, \nu_2 = 2$ (bottom). $\eta = 1$.

c. Sequential and hierarchical specialization

We provide figures that complement sections III A and III B, showing the specialization of the heads for an anisotropic Gaussian distribution. The four different runs show that the behaviour of the heads is similar across initializations.

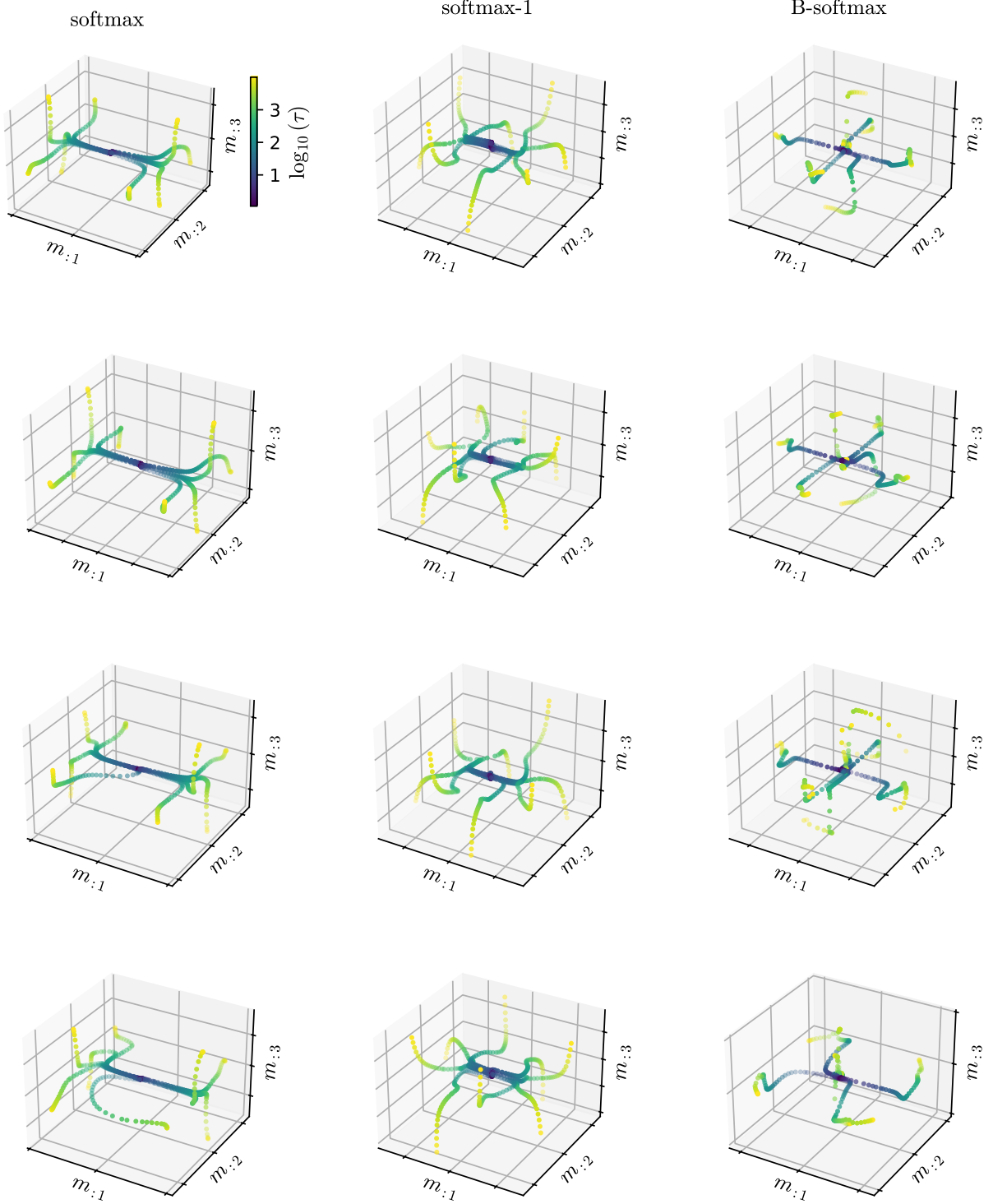


FIG. 19. Evolution of the $H = 8$ heads for the non-isotropic Gaussian distribution at $F = 3$. The four lines are four different runs with different initial conditions. The corresponding numerical values of m are shown in Fig. 20. $L = 5$, $\nu_1 = 20$, $\nu_2 = 1$ and $\eta = 1$.

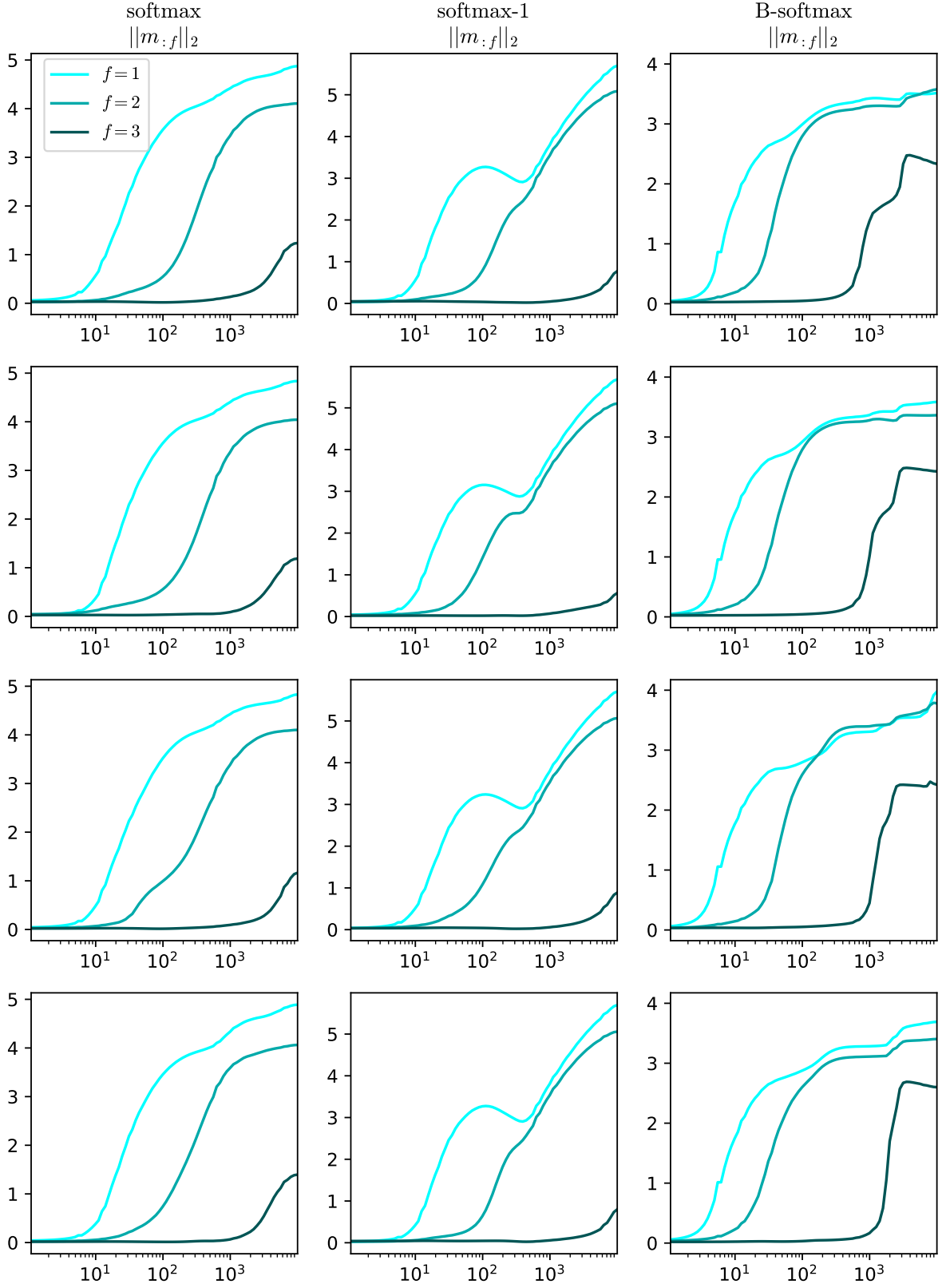


FIG. 20. Evolution of the $H = 8$ heads for the non-isotropic Gaussian distribution at $F = 3$. The four lines are four different runs with different initial conditions and correspond to Fig. 19. $L = 5$, $\nu_1 = 20$, $\nu_2 = 1$ and $\eta = 1$.